Assessment of Pulmonary Blood Flow in Heart Failure. Using Novel and Non-Invasive Diagnostic Methods.

Al-Mashat, Mariam

2021

Document Version:
Publisher's PDF, also known as Version of record

Assessment of Pulmonary Blood Flow in Heart Failure

Using Novel and Non-Invasive Diagnostic Methods

MARIAM AL-MASHAT
DEPARTMENT OF CLINICAL PHYSIOLOGY | FACULTY OF MEDICINE | LUND UNIVERSITY

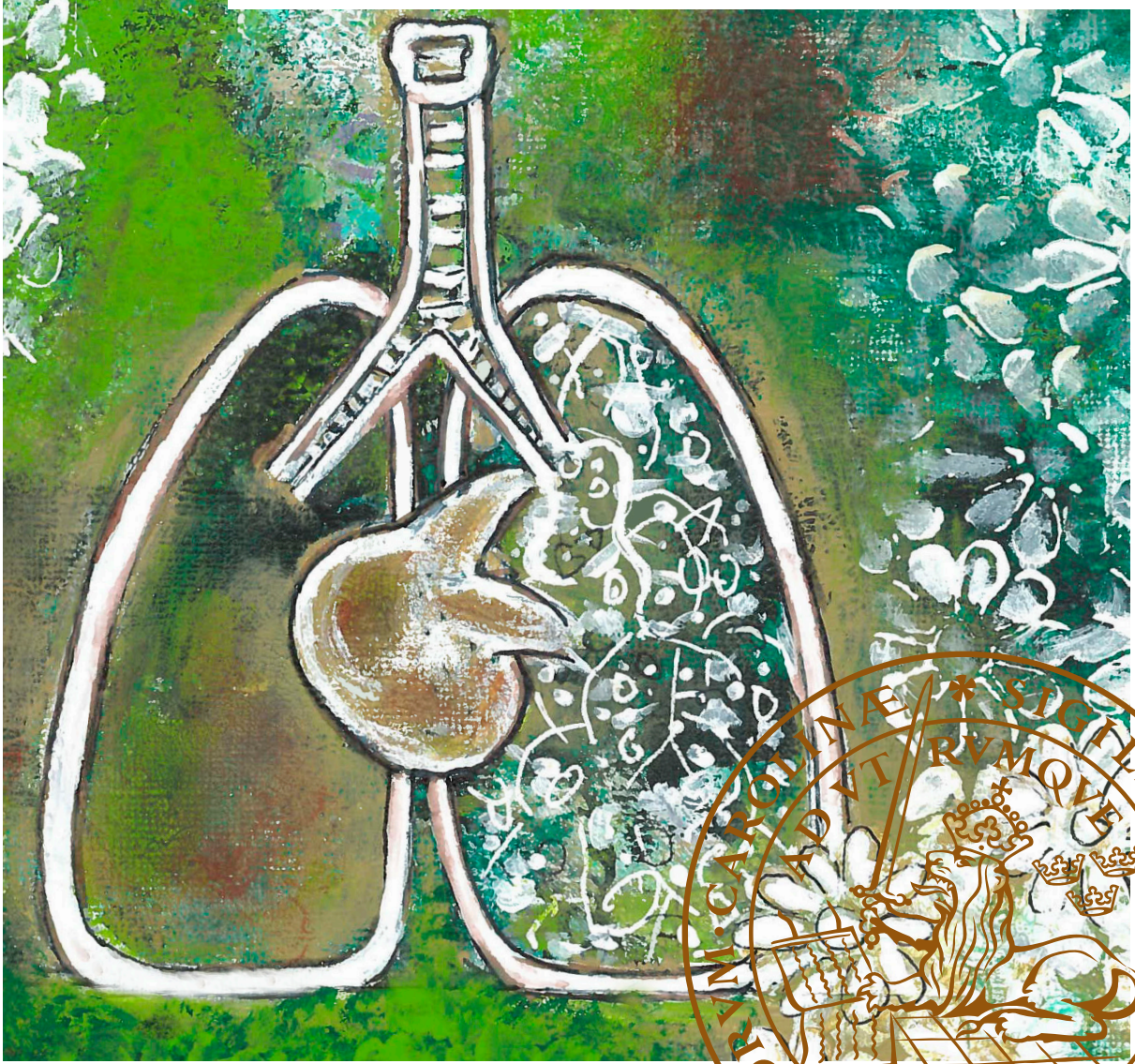

Assessment of Pulmonary Blood Flow in Heart Failure

Assessment of Pulmonary Blood Flow in Heart Failure

Using Novel and Non-Invasive Diagnostic Methods

Mariam Al-Mashat

LUND
UNIVERSITY

A doctoral thesis at a university in Sweden takes either the form of a single, cohesive research study (monograph) or a summary of research papers (compilation thesis), which the doctoral student has written alone or together with one or several other author(s).
In the latter case, which is the form of the present thesis, the thesis consists of two parts. An introductory text puts the research work into context and summarizes the main points of the papers. Then, the research publications themselves are reproduced, together with a description of the individual contributions of the authors. The research papers may either have been already published or are manuscripts at various stages (in press, submitted, or in manuscript).

Cover front: "Spring's breaths"
Artist: Mona Taqi

Cover back: The author of the thesis
Photographer: Sarah Khafagi

Typeset in LaTeX using a template by Berry Holl with modifications from Daniel Carrera

Lund University, Faculty of Medicine, Department of Clinical Physiology

ISBN: 978-91-8021-007-2
ISSN: 1652-8220
Lund University, Faculty of Medicine Doctoral Dissertation Series 2021:01

Printed in Sweden by Media Tryck, Lund University, Lund, Sweden, 2021

This thesis is dedicated to
- my parents,
- my husband & our miracles,
- my two brothers...

Indeed with hardship comes ease- Quran 94:6

Where there is a will, there is a way- Albert Einstein

It is the journey that makes you qualified for the destination- Hassan Al-Mashat

Contents

List of publications

The thesis is based on the studies presented in the following list, and will be referred to by their numeral numbers:

I **Diagnosing and grading heart failure with tomographic perfusion lung scintigraphy: validation with right heart catheterization.** J. Jögi, **M. Al-Mashat**, G. Rådegran, M. Bajc, H. Arheden. *European Society of Cardiology Heart Failure*, 2018;5(5):902-910. doi: 10.1002/ehf2.12317.

II **Deranged lung perfusion pattern in patients with heart failure normalizes after heart transplantation. M. Al-Mashat**, G. Rådegran, H. Arheden, J. Jögi. *Circulation Cardiovascular Imaging*, 2020;13(10):e011102. doi: 10.1161/CIRCIMAGING.120.011102.

III **Pulmonary perfusion gradients from tomographic lung scintigraphy improves in patients with heart failure after cardiac resynchronization therapy, and is associated with improved NYHA-classification. M. Al-Mashat**, R. Borgquist, M. Carlsson, H. Arheden, J. Jögi. *Manuscript*.

IV **Increased pulmonary blood volume variation in patients with heart failure compared to healthy controls: a noninvasive, quantitative measure of heart failure. M. Al-Mashat**, J. Jögi, M. Carlsson, R. Borgquist, E. Ostenfeld, M. Magnusson, E. Bachus, G. Rådegran, H. Arheden, M. Kanski. *Journal of Applied Physiology*, 2020;128(2):324-337. doi: 10.1152/japplphysiol.00507.2019.

My contributions to each paper are presented in the following table:

	Study design	Ethical application	Data collection	Data analysis	Statistical analysis	Figures and tables	Interpretation of the results	Preparation of manuscript	Revision of manuscript	Response to reviewers
Paper I	2	3	3	3	3	2	3	1	3	3
Paper II	2	3	3	3	3	3	3	3	3	3
Paper III	2	3	3	3	3	3	3	3	-	-
Paper IV	2	3	2	3	3	2	3	3	3	3

Not applicable	-
No contribution	0
Limited contribution	1
Moderate contribution	2
Significant contribution	3

Scientific publications not included in this thesis

Discrimination of ST deviation caused by acute coronary occlusion from normal variants and other abnormal conditions, using computed electrocardiographic imaging based on 12-lead ECG. S. Akil, **M. Al-Mashat**, B. Hedén, F. Hedeer, J. Jögi, JJ. Wang, GS. Wagner, JW. Warren, O. Pahlm, BM. Horáček. *Journal of Electrocardiology*, 2013;46(3):197-203. doi:10.1016/j.jelectrocard.2013.02.013.

The brain-enriched microRNA miR-124 in plasma predicts neurological outcome after cardiac arrest. P. Gilje, O. Gidlöf, M. Rundgren, T. Cronberg, **M. Al-Mashat**, B. Olde, H. Friberg, D. Erlinge.*Critical Care*, 2014;18(2):R40. doi: 10.1186/cc13753.

Automatic lung segmentation in functional SPECT images using active shape models trained on reference lung shapes from CT. GA. Cheimariotis, **M. Al-Mashat**, K. Haris, A H. Aletras, J. Jögi, M. Bajc, N. Maglaveras, E. Heiberg. *Annual Nuclear Medicine*, 2018;32(2):94-104. doi: 10.1007/s12149-017-1223-y.

Effect of exercise on the plasma vesicular proteome: a methodological study comparing acoustic trapping and centrifugation. P. Bryl-Górecka, R. Sathanoori, **M. Al-Mashat**, B. Olde, J. Jögi, M. Evander, T. Laurell, D. Erlinge. *Lab on a Chip*, 2018;18(20):3101-3111. doi: 10.1039/c8lc00686e.

The association between plasma miR-122-5p release pattern at admission and all-cause mortality or shock after out-of-hospital cardiac arrest. P. Gilje, M. Frydland, J. Bro-Jeppesen, J. Dankiewicz, H. Friberg, M. Rundgren, Y. Devaux, P. Stammet, **M. Al-Mashat**, J. Jögi, J. Kjaergaard, C. Hassager, D. Erlinge. *Biomarkers*, 2019;24(1):29-35. doi: 10.1080/1354750X.2018.1499804.

Abstract

In heart failure (HF), the heart is unable to pump effectively in order to satisfy the demands of the body. The elevated filling pressure seen in HF leads to accumulation of fluid in the lungs, i.e pulmonary congestion. While investigation with chest X-ray is recommended, it has limitations in detecting pulmonary congestion. Ventilation/perfusion single-photon emission computed tomography (V/P SPECT), i.e tomographic lung scintigraphy, is a promising method to diagnose and quantify pulmonary congestion in HF but needs to be validated by invasive right-heart catheterization. The variation of the blood volume in the pulmonary circulation measured by magnetic resonance imaging (MRI) may also have the potential to quantify the severity of HF. The general aim of this thesis was to develop and validate new non-invasive methods to diagnose and quantify pulmonary congestion and variation of the pulmonary blood flow in patients with HF, as well as to follow-up pulmonary congestion. **Paper I** revealed that the degree of pulmonary congestion in HF could be diagnosed and quantified using V/P SPECT. It was validated with right-heart catheterization. V/P SPECT was more accurate than chest X-ray in diagnosing pulmonary congestion in HF. In **Paper II** V/P SPECT showed that the pulmonary perfusion pattern was improved and that V/P SPECT could be used to follow treatment effect after heart transplantation in patients with HF and quantify the degree of pulmonary congestion. It was validated with right-heart catheterization. **Paper III** demonstrated that V/P SPECT could be used to follow treatment effect and assess the degree of pulmonary congestion in patients with HF after receiving cardiac resynchronization therapy (CRT). V/P SPECT was associated with improvement in patients' symptoms. **Paper IV** showed that the pulmonary blood volume variation differed between patients with HF and healthy controls. In patients with HF, approximately 40% of the variation could be explained by the left ventricular longitudinal contribution to stroke volume and the phase shift between the in- and outflow to the pulmonary circulation. The remaining variation (60%) likely occur on a small vessel level. **In summary,** pulmonary congestion in HF is difficult to quantify objectively. The non-invasive methods V/P SPECT and MRI might add complementary information in the diagnosis of HF. V/P SPECT can be used to follow treatment effects after heart transplantation and CRT and may have a role in avoiding invasive right-heart catheterization in selected cases and aid in treatment decision.

Populärvetenskaplig sammanfattning

Hjärtsvikt innebär att hjärtat inte pumpar tillräckligt med blod för att tillgodose kroppens behov. Vid hjärtsvikt ses ett ökat fyllnadstryck i hjärtat som kan leda till lungödem, ett tillstånd där vätska ansamlas i lungorna. Enligt riktlinjer undersöks detta med lungröntgen, men studier har visat att detta inte fungerar tillfredställande. Tomografisk lungscintigrafi är en lovande metod för att påvisa och kvantifiera graden av lungödem, men behöver valideras med hjärtkateterisering. Vidare kan man med magnetkamera (MR) undersöka hur mycket blodflödet i lungkretsloppet varierar, en metod för att kvantifiera graden av hjärtsvikt. Huvudsyftet med avhandlingen var att utveckla och validera nya icke-invasiva metoder för att diagnostisera och kvantifiera lungödem och variationen av blodflödet i lungkretsloppet hos patienter med hjärtsvikt, samt följa upp lungödem. **Delarbete I** visade att tomografisk lungscintigrafi kan diagnostisera och kvantifiera graden av lungödem vid hjärtsvikt. Metoden validerades med hjärtkateterisering. Vid jämförelse med lungröntgen var tomografisk lungscintigrafi bättre vid diagnostik av lungödem vid hjärtsvikt. **Delarbete II** visade att perfusionsmönstret i lungorna förbättrades hos hjärtsviktspatienter och kan användas för att följa behandlingseffekt efter hjärttransplantation, samt kvantifiera graden av lungödempåverkan, även här validerat med hjärtkateterisering. **Delarbete III** visade att tomografisk lungscintigrafi kan användas för att följa behandlingseffekten och mäta graden av lungödem hos hjärtsviktspatienter som fått en biventrikulär pacemaker för att synkronisera kamrarnas sammandragningar och öka pumpförmågan. Resultaten var också associerad med förbättring av patienternas symptom. **Delarbete IV** visade att variationen av blodflödet i lungkretsloppet mätt med MR kan skilja mellan patienter med hjärtsvikt och friska kontroller. Hos patienterna berodde ca 40% av variationen på att hjärtmuskelns förmåga att förkortas när den drar ihop sig, vilket leder till att blodet sugs till förmaket från lungvenerna, är nedsatt. Den berodde också på att tidpunkten där den maximala blodvolymsvariationen i lungorna inträffar senare än hos kontroller. Den resterande variationen (ca 60%) sker troligen på småkärlsnivå. **Sammanfattningsvis;** lungödem vid hjärtsvikt är en erkänt svår diagnos att kvantifiera objektivt. De icke-invasiva metoderna tomografisk lungscintigrafi och MR kan erbjuda kompletterande information vid hjärtsviktsdiagnostik. Tomografisk lungscintigrafi kan användas för att följa upp behandlingseffekten efter hjärttransplantation och biventrikulär pacemaker, samt ha en avgörande roll vid selektering av utvalda fall för en hjärtkateterisering och vara en hjälp vid beslutsfattande av behandling.

ملخص باللغه العربيه Arabic summary

العجزُ في عضلةِ القلبِ يُؤدي الى عدمِ انتقالِ الدمِ بالكميةِ المطلوبةِ وبشكلٍ طبيعي إلى سائر أعضاءِ الجسمِ .. وبالتالي ، فإنّ ضغطَ تعبئة القلبِ بالدَّمِ عندَ عجزِهِ يصبحُ عالياً ويؤدّي إلى تراكمِ السوائلِ في الرئتينِ .. ووفقاً للإرشاداتِ الحاليةِ ، فإنَّ فحصَ هذهِ الحالة يتمُّ بواسطة الأشعةِ السينيةِ للصدر .. ولكنّ الدراساتِ أثبتت أنَّ هذا الفحصَ لا يُعطي نتائجَ مرضيةً .. وعليه فإنّ التصوير النووي للرئة هو فحصٌ واعدٌ لتحديدِ كميةِ تراكمِ السوائلِ في الرئتين عندَ المرضى الذين يعانونَ من عجزٍ في عضلة القلبِ .. وقبلَ كلِّ شئ يجبُ التحققُّ من ذلك بعد قسطرةِ القلبِ لأنَّ هذا الفحصَ هو الفحصُ القياسي لمعرفةِ تراكمِ السوائلِ في الرئتينِ ، ويلي ذلك الفحصُ بالرنين المغناطيسي للقلبِ لمعرفةِ درجةِ العجزِ فيه .. لقد أظهرَت نتائج **البحثُ الاولُ** في هذه الأطروحةِ أنّ الفحصَ التصويري النووي للرئةِ يستطيعُ أنْ يُحدِّدَ كميةَ تراكمِ السوائلِ في الرئتينِ عندَ المرضى الذين يعانونَ من عجزٍ في عضلةِ القلبِ .. وعلى هذا الأساسِ فإنّ الفحصَ التصويري النووي للرئةِ هو أفضلُ من الفحصِ بالأشعةِ السينيةِ للصدرِ لمعرفةِ كميةِ تراكم السوائلِ في الرئتينِ عندَ مقارنةِ نتائجِ الفحصين مع نتائج قسطرةِ القلبِ .. وأظهر **البحثُ الثاني** إمكانيةَ استخدامِ الفحصِ النووي للرئةِ لتحديدِ كميةِ تراكمِ السوائلِ فيها عندَ المرضى الذين يعانونَ من عجزٍ في عضلة القلبِ ؛ ولتتبعِ نتائجُ العلاجِ بعدَ زراعةِ القلبِ .. عند مقارنةِ نتائجِ الفحصِ النووي للرئةِ مع نتائجِ قسطرهِ القلب .. ولقد أظهرَ **البحثُ الثالثُ** في هذهِ الاطروحةِ إمكانيةَ استخدامِ الفحصِ النووي للرئةِ لمعرفةِ نتائجِ العلاجِ بعدَ زرعِ جهازِ تنظيمِ ضرباتِ القلبِ عندَ المرضى الذين يعانونَ من عجزٍ في عضلة القلبِ ولتحديدِ كمّيةِ تراكمِ السوائلِ في الرئتينِ ؛ وكانت هذهِ النتائجُ مرتبطةً بأعراضِ عجزِ عضلة القلبِ .. وأما **البحث الرابع** ، فأظهرت النتائجُ أنّهُ عندَ استخدامِ التصوير بالرنين المغناطيسي للقلبِ ، فإنَّ كميةَ اختلافِ تدفّقِ الدمِ في الدورةِ الدمويةِ للرئةِ عندَ مرضى عجزِ عضلةِ القلبِ كانتْ أعلى من الاصحاء بحوالي ٤٠٪ ، وإنَّ هذا الاختلافَ عندَ المرضى سببُهُ هو ضعفُ عضلةِ القلبِ عندَ الانقباضِ ، وإن الوقتَ الذي يتمُّ فيهِ تفريغُ الدمِ من الرئةِ ، ودخولَ الدمِ إليها يحدثُ لاحقاً .. أمّا النسبة المتبقّيةُ ، فهي حوالي ٦٠٪ ، ويُعزى هذا الاختلافُ إلى تدفّقِ الدمِ في الأوعية الدموية الصغرى .. **خلاصه الأطروحة** إنّ العجزَ في عضلةِ القلبِ تشخيصٌ يصعبُ تحديدّهُ .. فإنّ التصويرَ النوويُ للرئةِ والتصويرَ بالرنين المغناطيسي للقلبِ ، والذي يُعتبر من الفحوصاتِ الجديدةَ غير الجراحية ، يضيفان معلوماتِ تكميليه لتشخيصِ العجزِ في عضلةِ القلبِ .. وقد أثبتتِ البحوثُ أنهَ من الممكنِ استخدامُ التصويرِ النووي للرئةِ لمتابعةِ العلاجِ بعد زراعهِ القلبِ وبعد زراعةِ جهازِ تنظيمِ ضرباتِ القلبِ ، وله دور مهم عند اختيارِ حالاتٍ محددةٍ لخضوعِ المريضِ لقسطرةِ القلبِ وفي تحديد نوعِ العلاجِ ..

Acknowledgements

The journey towards accomplishing my dream of obtaining a PhD degree has been many years long. Yet it has been a journey that I experienced and learned way more than I ever would have imagined, and that I will not forget and will bring with me for the rest of my life. This journey was filled with joy, tears, and hope and it would not have been able to take place without the help of several persons. Therefore, I would like to express my greatest thankfulness to the following persons:

My supervisors; **Jonas Jögi** and **Håkan Arheden**. Thank you **Jonas**, for always finding time for meetings (despite you having no time for research), for your immense knowledge, and great discussions. Thank you for your support, teaching me independence and for believing in me. Thank you **Håkan**, for accepting my request of starting my PhD studies that day I knocked on your door many years ago. Thank you for teaching me acceptance and that life is all about choices, which helped me to take the best choice of my life. Thank you for always asking questions, believing in me, and teaching me leadership.

My supportive colleague, **Mikael Kanski**, thank you for all the hard work with paper IV and for sharing all your knowledge in this field. My former clinical boss, **Lisbeth Nilsson**, thank you for your kindness and support in all my academic studies, for always finding solutions for everything and for your endless support. My current clinical boss, **Eva Fabricius**, thank you for continuing the same path and for your kindness, understanding and support.

Olle Pahlm, thank you for introducing me to the world of research, for the possibility to attend my first conference ever and for publishing my first paper, prior to my PhD studies. My dearest friend and former colleague, **Shahnaz Akil**, thank you for all your endless support and wise advices in everything, and for always answering my questions. We have gone through many things in life together in which I'm very grateful for. **Marcus Carlsson**, thank you for always having time and answers for short questions, and for all the great discussions about physiology. Thank you **Katarina Steding-Ehrenborg**, for all our discussions about physiology, for being such a huge support and inspiration and for giving me hope.

Anders Nelsson, thank you for our common interest in V/P SPECT and heart failure, and for great cooperation in the inclusion of patients. **Johannes Töger**, thank you for all the help with Latex and for being an inspiration. **Sebastian Johansson**, thank you for your knowledge in MRI. All the **PhD students** in the chamber, thanks for everything and good luck with your journeys. **Barbro Kjellström**, thank you for all of the great discussions, questions, and feedback and for being such an inspiration. It feels that we have known each other for many years. **Ellen Ostenfeld, Erik Hedström, Anthony Aletras, Einar Heiberg,** and **Henrik Engblom**, thank you for being an inspiration. **Jane Tufvesson**, thank you for being who you are in the Lund Cardiac MR group. **Felicia Seemann** and **Marjolein Piek** thank you for your friendship and support during my PhD journey. To all the other members in the Lund Cardiac MR group, thank you for the support.

Department of Clinical Physiology and Nuclear Medicine in Lund: all my technologist colleagues in the clinic in **enhet 1**, thank you for your support. All my technologist colleagues in **enhet 2** who performed the V/P SPECT examinations, thank you! Special thanks to **Frida Johansson** and **Stefan Sierra Johansson** for your help in patient inclusion during my parental leave. All my colleagues who performed the MRI examinations: **Ann-Helen Arvidsson, Christel Carlander, Charlotte Åkesson, Johanna Koul** and **Reza Farazdaghi**, thank you!

All my co-authors in the papers: **Marika Bajc, Göran Rådegran, Rasmus Borgquist, Martin Magnusson** and **Erasmus Bachus**, thank you for the fruitful cooperation. All the patients and healthy controls included in the papers, thank you for your participation.

To all my friends, thank you for believing in me. Special thanks to **Jasmina, Sarab,** and **Sarah**, for taking part of the photoshoot of my portrait in the back cover of the thesis. Thank you, **Sarah**, for taking the photo.

All my relatives and cousins in Sweden and all over the world, thank you for believing in me. Special thanks to my aunt and artist, **Mona Taqi**, for the most beautiful drawing in the front cover of this book. Thank you my aunt Mona and my dear cousin **Zainab Alsaffar** for your feedback in the Arabic summary of the thesis.

My parents: my father **Shaker** and my mother **Weam**, there are no words that could express my greatest sincere to you, if there was then I would have said them endless times. Thank you for always offering a caring and loving environment for me and my brothers to be raised in, always supporting our choices in life and for teaching us kindness. Thank you for facilitating every step in my life so I can finish this PhD journey and for believing in me. I am forever grateful. My brother **Dolfakar** and my sister-in-law **Alexandra**, thank you for always offering your help in taking care of my son so I can attend meetings and finish my studies.

My brother **Hassan**, thank you for your endless support and for being the one that knows what I have been through in this journey and for believing in me, keep doing what you can so you can reach your dreams.

My father-in-law **Mohammad Reza**, and mother-in-law **Taghrid**, thank you for always believing in me, for supporting me, welcoming me into your family as one of your daughters, and for always taking care of my son during our visits so I could have meetings and finish parts of this journey. Special thanks to my father in-law for putting the final touches on the Arabic summary of this thesis. My sisters-in-law: **Hoda, Alieh,** and **Esra**, I can't thank you enough for always offering your help in taking care of my son during our visits so I could have meetings and work with parts of my PhD studies and for believing in me.

My dearest husband **Ali**, my comfort zone, and my everything, thank you for always supporting me, for believing in me and always telling me that this journey will come to an end even during days when I didn't see that coming, and our son **Mohamad**, thank you for your endless love and for your patients during my studies. The two of you and the sibling that is on the way are my biggest treasure in this world which I do not want to replace with anything else… I love you all and you mean everything to me.

Thank you **God**, for all your guidance through this journey and for everything in my life.

Malmö, November 11th, 2020

Preface

It was my dream to become a Biomedical scientist (Technologist) and reach a PhD degree already back in high school. My first contact with the Department of Clinical Physiology and Nuclear Medicine at Skåne University Hospital in Lund was when I performed my extended clinical training there during my third and last year at the Biomedical scientist program (with clinical physiology as specialty) at Malmö University. I was very lucky that the research group, Lund Cardiac MR group, is a part of this department because that meant that I was not far away from reaching my dream. I performed my bachelor and master thesis at the same department. While performing my last year in the master's studies (from Örebro University, Sweden) and working simultaneously in the clinic, I started to plan the journey towards my PhD, which I still am very thankful to have been able to perform at the department.

This thesis was performed under the supervision of Ph.D. Jonas Jögi and professor Håkan Arheden.
I was very interested in research, especially research related to the heart and lungs. The design of my thesis projects enabled me to work with both the heart and lungs. The inclusion of patients in this project was a time-consuming process, but in the end, it resulted in a unique patient population. The present thesis is about assessing the pulmonary blood flow in patients with heart failure using novel and non-invasive diagnostic methods; ventilation/perfusion single-photon emission computed tomography and magnetic resonance imaging.
During my time as a PhD student, I worked in the clinic, attended conferences, supervised students, and met many patients who I included in my project. The possibility to really be part of the project from the very beginning, resulted in me acquiring good skills in this field.

The studies in this thesis were funded by the Swedish Heart Lung Foundation, ALF Medical Faculty grants at Lund University and the Swedish Research Council. The travel grants were funded by the Swedish Society for Clinical Physiology, Scandinavian Society of Clinical Physiology and Nuclear Medicine, the Swedish Heart Lung Foundation and Lund University.

Thesis at a glance

Thesis at a glance			
Title	**Aim**	**Main results**	**Conclusions**
Paper I: Diagnosing and grading heart failure with tomographic perfusion lung scintigraphy: validation with right heart catheterization.	To 1) evaluate the potential of V/P SPECT as a non-invasive method to assess and quantify pulmonary congestion in patients with heart failure using right-heart catheterization as reference method, 2) investigate the performance of V/P SPECT compared with chest X-ray in the clinical setting.	The sensitivity for V/P SPECT (by expert reader) in the assessment of pulmonary congestion was 87%, whereas it was 27% in the clinical assessment of chest X-ray. The majority of patients with elevated PAWP also had abnormal V/P SPECT, and patients with normal PAWP had normal V/P SPECT.	V/P SPECT can be used as a non-invasive method to diagnose and quantify pulmonary congestion in patients with heart failure and is more accurate than chest X-ray in diagnosing pulmonary congestion in the clinical setting.
Paper II: Deranged lung perfusion pattern normalizes in patients with heart failure after heart transplantation.	To investigate if V/P SPECT can be used to assess treatment effect after heart transplantation using right-heart catheterization as the reference method.	V/P SPECT and PAWP were improved and normalized after heart transplantation. There was a correlation between V/P SPECT and PAWP and a discrimination can be made between normal and abnormal results.	V/P SPECT is a promising method for objective assessment and quantification of treatment effects in patients with heart failure after heart transplantation and could be a non-invasive and useful method in selected cases to guide treatment and catheterization during follow-up.
Paper III: Pulmonary perfusion gradients from tomographic lung scintigraphy improves in patients with heart failure after cardiac resynchronization therapy, and is associated with improved NYHA-classification.	To assess if changes in perfusion gradients from V/P SPECT are associated with improvement in heart failure symptoms after CRT. In addition, to evaluate if perfusion gradients from V/P SPECT correlate to currently used methods in the follow-up of patients with heart failure after receiving CRT.	The majority of the patients improved in perfusion gradients from V/P SPECT after CRT (68%) compared to LVESV from echocardiography (37%). Improvement in perfusion gradients was associated with improvement in NYHA-classification, n=11/13 (85%), p=0.0456.	Improvement of perfusion gradients was shown in a larger proportion of the patients after CRT compared to echocardiography. Improved perfusion gradients were associated with an improvement of patients' functional capacity, according to NYHA. Perfusion gradients could have an added value to the currently used diagnostic methods in the follow-up of patients with heart failure after receiving CRT.
Paper IV: Increased pulmonary blood volume variation in patients with heart failure compared to healthy controls: a noninvasive, quantitative measure of heart failure.	To evaluate whether PBVV differs in patients with heart failure compared with healthy controls and investigate the mechanisms behind the PBVV.	Patients with heart failure had higher $PBVV_{SV}$ compared to healthy controls. This could be explained by LV contribution to SV and the phase shift between in- and outflow. Both variables predicted $PBVV_{SV}$ in a multiple regression analysis model with R^2=0.38.	$PBVV_{SV}$ was higher in patients compared with controls. Approximately 40% of the variation of $PBVV_{SV}$ in patients can be explained by the LV longitudinal contribution to SV and the phase shift between pulmonary in- and outflow. The remaining variation (60%) most likely occurs on a small vessel level.

Abbreviations: tomographic lung scintigraphy = also referred to as V/P SPECT (ventilation/perfusion single-photon emission computed tomography); PAWP = pulmonary artery wedge pressure; CRT = cardiac resynchronization therapy; NYHA = New York Heart Association; LVESV = left ventricular end-systolic volume; PBVV = pulmonary blood volume variation; SV = stroke volume; LV = left ventricular

Abbreviations

AV	atrioventricular
AVPD	atrioventricular-plane displacement
CO	cardiac output
CRT	cardiac resynchronization therapy
ECG	electrocardiogram
ED	end-diastole
EDV	end-diastolic volume
EF	ejection fraction
ES	end-systole
ESV	end-systolic volume
HR	heart rate
IQR	Interquartile range
LAP	left atrial pressure
LV	left ventricle/left ventricular
LVAVPD	left ventricular atrioventricular-plane displacement
LVEF	left ventricular ejection fraction
LVESV	left ventricular end-systolic volume
MAA	macro-aggregated human albumin
MLWHF	minnesota living with heart failure
MR	magnetic resonance
MRI	magnetic resonance imaging
NPV	negative predictive value
NYHA	new york heart association
PAWP	pulmonary artery wedge pressure
PBVV	pulmonary blood volume variation
PPV	positive predictive value
RF	radio frequency
RV	right ventricle/right ventricular
SV	stroke volume

TE	echo time
TR	repetition time
VENC	velocity encoding gradient
V/P SPECT	ventilation/perfusion single-photon emission computed tomography
2D	two-dimensional
3D	three-dimensional
99mTc	99mTechnetium

Part I

Research context

Chapter 1

Introduction

The most essential and astonishing organ in the human body is the heart. The heart starts to beat very early in the fetal development and never stops beating until we die. The heart is therefore fundamental for living. Heart failure, on the other hand, leads to the inability to deliver enough oxygen to the body [1] [1]. It is a condition where not only the heart is affected, but also the lungs [1] [2] as well as other parts of the body such as the skeletal muscles [3].

1.1 Basic anatomy of the heart and lungs

The heart

The human heart is a muscle, divided into a right and left side with four chambers, see Figure 1.1. On both sides, there is one atrium and one ventricle. The main function of the atrium is to receive the blood coming back to the heart, and the main function of the ventricles is pumping and ejecting the blood. The left and right side are separated with a wall, the septum. The plane that separates the atria and ventricles is named atrioventricular (AV)-plane, where the valves are attached. The valve on the left side is the mitral valve, and the valve on the right side is the tricuspid valve. Inferior and superior Vena cava takes the blood coming from the lower and upper parts of the body to the right atrium. On the right side, blood is ejected from the right ventricle (RV), through the pulmonary valve, to the lungs. The blood thereafter returns to the left side of the heart through pulmonary veins. From the left ventricle (LV), blood is ejected into the systemic circulation through the aortic valve.

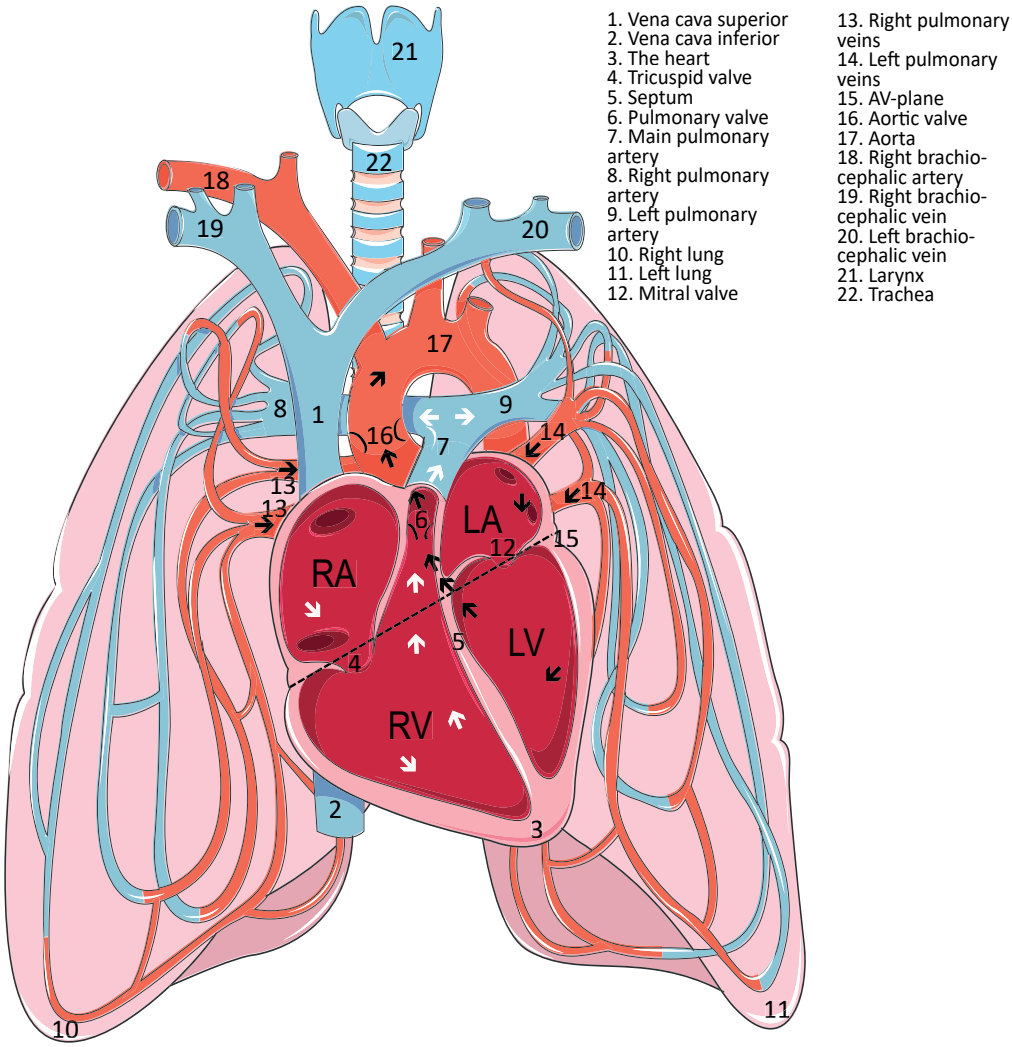

Figure 1.1: Image of the heart, lungs, the pulmonary and parts of the systemic circulation. White arrows shows blood flow on the right side of the heart delivering blood to the pulmonary circulation. Black arrows shows blood flow on the left side of the heart, delivering blood to the systemic circulation. RA; right atrium, RV; right ventricle, LA; left atrium, LV; left ventricle.
Image modified and used with permission from Servier Medical Art - Creative Commons Attribution 3.0 Unported Licence.

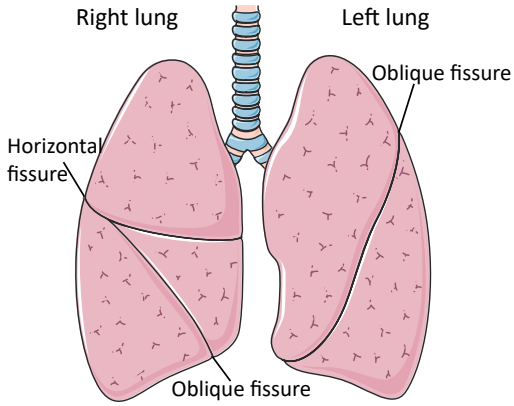

Figure 1.2: Image of the right and left lung. There are three lobes in the right lung, and two in the left. *Image modified and used with permission from Servier Medical Art - Creative Commons Attribution 3.0 Unported Licence.*

The lungs

The human body has two lungs, one on each side, see Figure 1.2. Both the right and left lung are divided into lobes; three on the right and two on the left side. The superior part of the lungs is called the apex, and the lung base is the inferior part. Hilum is a location in the lungs where arteries, veins, lymph vessels, and nerves enter and leave the lungs. The heart is in close proximity to the left lung; which makes the right lung larger than the left. The lobes of the right lung are separated with both horizontal and oblique fissures, whereas the lobes on the left lung are separated with only an oblique fissure.

The lungs are surrounded by a sack named pleura. The pleura is located between the thorax wall and the lungs. Pleura has two layers. The inner layer is the visceral pleura which is attached to the lungs, and the outer layer is the parietal pleura which is attached to the chest wall. Between them is the pleural space containing pleural fluid.

Air enters the lungs through the nose and mouth during inspiration, which continues into larynx and trachea (the beginning of the bronchial tree), as seen in Figure 1.3. The trachea is subdivided to one right and one left primary bronchus. The subdivision continues into secondary bronchi for each lobe of the lungs, which is further branching into tertiary bronchi (smaller bronchi). This is then divided into bronchioles. These bronchiole structures are in the **conducting zone** where there are no vessels and blood. The bronchioles are subdivided to terminal bronchiole, which in turn are split to respiratory bronchioles. The subdivision of the respiratory bronchioles continues and terminates into numerous alveolar ducts and sacs (two or more alveoli share one duct). These structures are in the **respiratory zone**, and the alveoli are supplied with a network of blood, capillaries, where the gas exchange between the blood and air take place. The pulmonary gas exchange occurs in the **alveoli**.

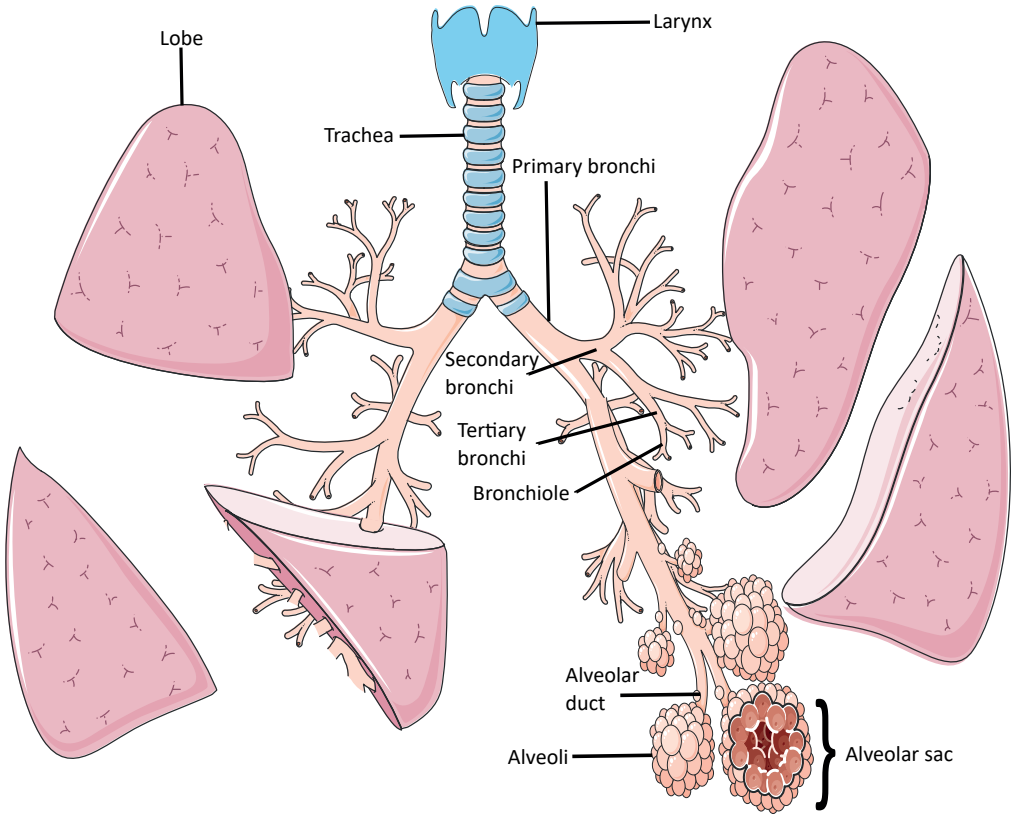

Figure 1.3: Image of the right and left lung with the corresponding lobes and bronchial tree. The bronchial tree consists of primary-, secondary-, tertiary bronchies, bronchiole, alveolar duct, alveoli and small alveolar sacs. The open part of the sacs is connected to the rest of the airways.
Image modified and used with permission from Servier Medical Art - Creative Commons Attribution 3.0 Unported Licence.

Pulmonary vessels
- **Pulmonary arteries** are divided into a left and right main branch from the pulmonary artery (Truncus pulmonalis) and supplies both lungs with desaturated blood.

- **Pulmonary veins** return the saturated blood back from the lungs to the left atrium. There are usually four pulmonary veins (two on each side). However, this can differ between persons.

- **Bronchial vessels** are small bronchial arteries that originates from the systemic circulation. These arteries also supply the lungs (including the small and large bronchi, septum and connecting tissue) with oxygenated blood. Thereafter, the blood from the bronchial vessels and arteries enter the left atrium through the pulmonary veins.

- **Lymph vessels:** are located in the supportive tissues of the lungs starting from the terminal bronchioles, and terminates mainly in the right thoracic lymph duct, passing the hilum [4]. These vessels are the ones that help in preventing pulmonary edema by eliminating the leakage of plasma protein from the capillaries in the lungs.

1.2 The cardiopulmonary system

The cardiopulmonary system consists of the cardiovascular system and the pulmonary system.

1.2.1 The cardiovascular system

The cardiovascular system consists of the heart, the pulmonary- and systemic circulation, see Figure 1.1. The pulmonary circulation starts when deoxygenated blood in the right atrium flows through the tricuspid valve into the RV. From there, the blood is ejected through the pulmonary valve, via the pulmonary trunk (main pulmonary artery) and pulmonary arteries, to the lungs where the blood gets oxygenated. The oxygenated blood leaves the lungs via the pulmonary veins and enters the left atrium. From the left atrium, the blood continues through the mitral valve to the LV, from where it is ejected into the aorta through the aortic valve. From the aorta, the blood is delivered to the rest of the body.

The pressure in the pulmonary circulation is low (25/10 mmHg [5]), which results in a thin RV wall. On the other hand, the pressure in the systemic circulation is higher (120/80 mmHg [5]), which result in a thicker LV wall, compared to the RV wall. This is in order to overcome the higher pressure in the aorta and eject the blood.

1.2.2 Pulmonary physiology

The pulmonary system in the human body is essential. Its main functions are supplying the body with oxygen, helping the immune system, and eliminate carbon dioxide through ventilation. **Diffusion** is the exchange of carbon dioxide and oxygen between the blood and air in the alveoli.

Pulmonary ventilation is the exchange of air between the alveoli and the atmosphere (inspiration and expiration). The air flows in through airways and into the lungs during inspiration due to that the pressure in the alveoli is lower than the pressure in the atmosphere. During expiration, the pressure in the alveoli exceeds the pressure in the atmosphere, resulting in air flows out of the lungs. The regional ventilation in the lungs is dependent on the lung's local expansibility or elasticity. Under normal circumstances, the ventilation is more distributed to the lower parts of the lungs due to the larger compliance in those parts of the lungs.

Pulmonary perfusion. During normal conditions, the perfusion (blood) is distributed in the lower parts of the lungs (base) when standing and to the posterior/dorsal parts of the lungs while lying in supine position. This is because of the gravitation.
We can think of the large pulmonary vessels as rubber tubes that are elastic and can distend with changes in pressure. When the pressure is decreased, the pulmonary vessels reduce in diameter, and when the pressure is elevated, they are distended [4].
In order for the blood to be mixed with air, the blood in the lungs should be disseminated to the parts or segments of the lungs (alveoli) that have the most oxygen supply.
Accumulation of fluid in the interstitial space can cause mismatch between the ventilation and perfusion by compressing the blood vessels and small airways [6] [7].

The zones of the lungs
When the blood pressure in the pulmonary capillaries becomes lower than the alveolar air pressure of the lungs, the capillaries close resulting in no blood flow running through them. As described by West et al. [8] (and presented in Figure 1.4) the lungs are divided into different zones, based on the distribution of the blood flow (perfusion).

Zone I: The capillaries in zone I (the apical parts of the lungs) are not perfused and there is limited gas exchange. This is caused by the pulmonary arterial pressure being lower than the alveolar pressure, which at the same time is higher than the venous pressure, Figure 1.4. This means that during normal conditions, the lungs are foremost perfused in the lower parts, zone II and III.

Zone II: Consists of the middle parts of the lungs. Here in this zone, the pulmonary arterial pressure is larger than the pulmonary alveolar pressure, and the pulmonary alveo-

lar pressure is greater than the pulmonary venous pressure. The closer we get to zone III, the basal parts of the lung, the more capillaries are open with gradually more gas exchange taking place.

Zone III: Consists of the lower parts of the lungs. In this zone, the capillaries are constantly kept open since the pulmonary arterial pressure is larger than the alveolar pressure, and the alveolar pressure is lower than the venous pressure. Most of the gas exchange occurs in this zone.

Sometimes, a fourth zone at the base of the lungs is added to the three mentioned zones (**Zone IV**) [9]. In zone IV, the pressure in the lung tissue (the interstitial pressure) is larger than the pulmonary arterial, venous and alveolar pressures. In this zone, which is in the bottom (base) of the lung, the elevated interstitial pressure leads to a decreased perfusion again, which leads to atelectatic (or edematous) lung.

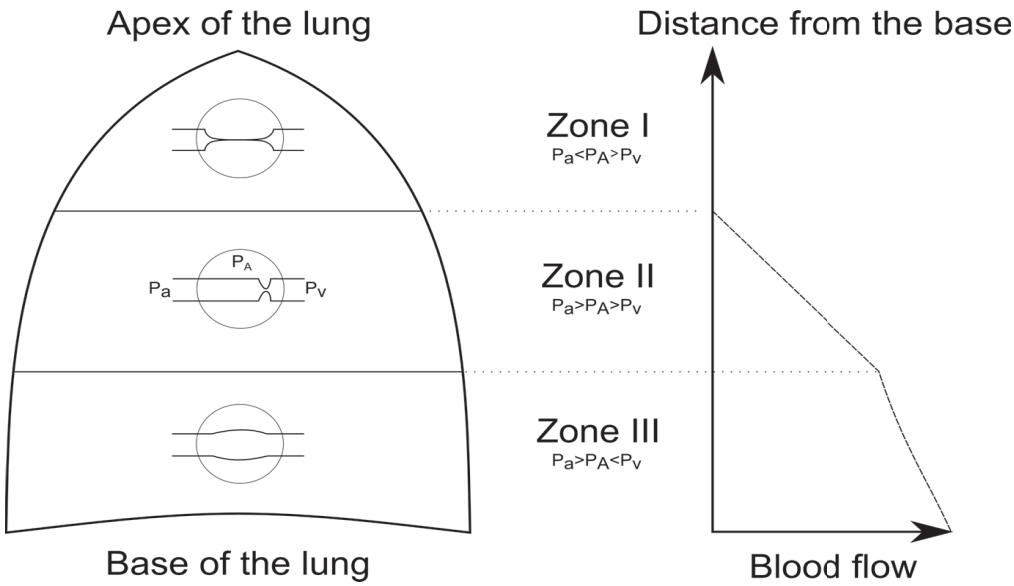

Figure 1.4: Schematic image of the lung in standing position with the corresponding blood flow. The lung is divided in three different zones [8], where the circle in each zone represents the alveoli and the capillaries inside of them. There is no blood flow in Zone 1 (the capillaries are closed), while in Zone III the capillaries are open and blood flow through them. P_a= arterial pressure, P_A= alveolar pressure, P_V= venous pressure. *Adapted with permission from Mikael Kanski* [10].

1.3 Pumping of the healthy heart

The cardiac cycle consists of two phases; systole and diastole. **Systole** is the phase where the ventricles are contracting and ejecting the blood to the rest of the body. **Diastole** is when the ventricles are filled with blood and relaxed. There are three different parts in diastole: early rapid filling, diastasis and atrial contraction.

During the beginning of the cardiac cycle, the atria are contracting. The pressure in the LV is lower than the pressure in the left atrium. This pressure gradient enables blood to flow in to the ventricle due to the opening of the AV valves. The atrial contraction provides an extra volume of blood into the LV before it starts to contract. When the pressure in the LV becomes greater than the pressure in the left atrium this will result in closure of the mitral valves (the isovolumetric contraction phase). When the ventricles contract, the AV-plane is moved towards the apex of the heart, the aortic valve opens, and blood is ejected to the body. The remaining blood volume in the end of systole (end of this phase) is named end-systolic volume, ESV.

Diastole begins with an isovolumetric relaxation that lead to a decreased LV pressure. Early rapid filling starts when the pressure in the LV is lower than the pressure in the left atrium and the AV valves opens. During this phase blood flows from the atrium to the ventricle. Diastasis is the next phase in diastole, where there is a small volume of blood that pass through the AV valves. Atrial contraction marks the end of diastole. The blood volume in the end of diastole is called end-diastolic volume, EDV.

The volume ejected by the heart in one heart beat is called stroke volume and can be calculated as:

$$SV = EDV - ESV \tag{1.1}$$

where SV is stroke volume, EDV is end-distolic volume and ESV is end-systolic volume. The volume of blood delivered to the systemic circulation per minute, in order to meet the metabolic demands of the tissues is called cardiac output. Cardiac output is calculated as:

$$CO = SV \cdot HR \tag{1.2}$$

where CO is cardiac output, SV is stroke volume and HR is heart rate.

In a healthy person at rest, CO is typically 5 l/min [5]. However, when the heart fails and is unable to deliver an adequate CO, we call it heart failure.

1.4 Heart failure

Heart failure is a complex clinical syndrome which is challenging to diagnose [1]. The prevalence of heart failure is 1-2% [11], which is more than 23 million people world-wide [12]. The prevalence continually rises as the population become older [11] [13]. Annually, cardiovascular disease causes over 3.9 million deaths in Europe [14] and 17.9 million deaths worldwide [15].

1.4.1 Pathophysiology

Heart failure is caused by any functional or structural impairment of ventricular filling or ejection of blood, which in itself can give rise to increased pressures in the heart. The causes include ischemic heart disease, coronary artery disease, hypertension, and pulmonary disease with pulmonary hypertension.

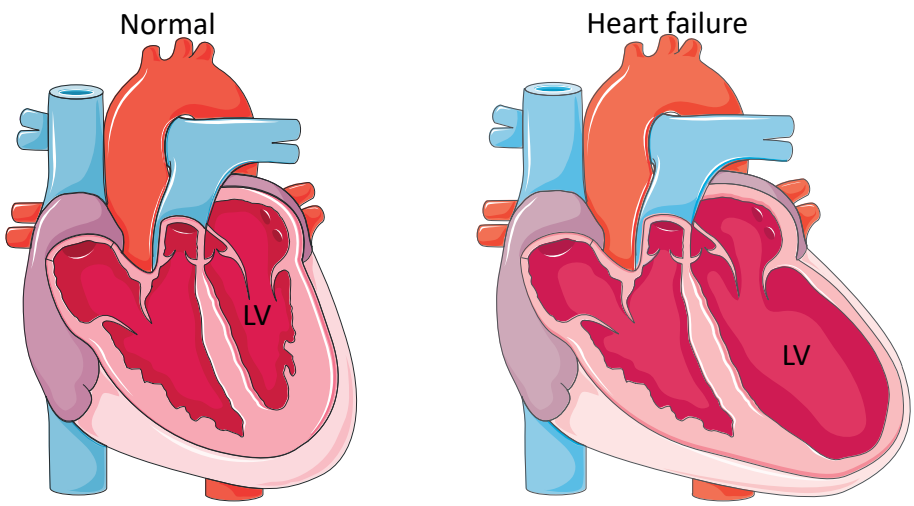

Figure 1.5: Image of the heart during normal condition (to the left) and during heart failure (to the right). Note how the left ventricle (LV) can be dilated in heart failure.
Image modified and used with permission from Servier Medical Art - Creative Commons Attribution 3.0 Unported Licence.

Heart failure can be divided into asymptomatic, chronic, stable, acute and congestive [1] [16]. Asymptomatic heart failure includes patients with no symptoms or signs, whereas chronic heart failure includes patients who have suffered from heart failure during a period of time [1] [16]. Patients with stable heart failure have unchanged signs or symptoms during at least one month, despite treatment. Patients with acute heart failure, also referred to as decompensated, experience a state where their chronic or stable heart failure is worsened [1] [17]. This state is serious, requires fast treatment and could affect the prognosis of the

patient. Chronic and acute heart failure can also be described as congestive heart failure [1].
There are different types of heart failure and these may have different manifestations. There is systolic and diastolic heart failure that can appear in the left and right side of the heart, thereby left and right-sided heart failure [1]. The consequences of heart failure can end in backward and forward failure. The focus in this thesis will be on systolic heart failure, left-sided heart failure and backward failure:

- Systolic heart failure. Ejection fraction (EF) is a measure of LV pumping (systolic function) [18], and is normally $\geq$ 50% [1]. EF can be calculated and measured using the following formula:

$$EF = \frac{(EDV - ESV) = SV}{EDV} \tag{1.3}$$

Systolic heart failure is a condition where the LV has reduced contractility and pumping/ejection of the blood. Patients with systolic heart failure have therefore reduced EF, $<$40% [1] and has shown to have increased mortality [19]. A common mechanism leading to systolic heart failure is following a myocardial infarction [20]. In surviving myocytes, a pathophysiological remodelling of the LV could occur. This could affect the LV by impairing its contractility and lead to dilation, see Figure 1.5.

The Frank Starling mechanism describes the association between the heart's systolic and diastolic function. The principle behind the Frank Starling mechanism [21] [22] [23] is that during diastole, when the ventricles are filled with blood, the cardiac muscles are stretched. The more the heart muscles are stretched the higher the force of contraction and SV during systole. Therefore, if the venous return to the heart is less the force of contraction, likewise become less. One of the causes to systolic heart failure is myocardial infarction. The part of the myocardium that is affected by the infarction, dies. This tissue will become fibrotic and will not have the ability to contract. This will therefore result in decreased starling force.

- Left-sided heart failure. Usually systolic heart failure affects the LV and causes left-sided heart failure. It is most commonly caused by ischemic heart disease.
As mentioned in section 1.2.1, the LV wall is thick since it is required to pump with a high pressure to overcome the pressure in the aorta and eject blood. In the case of left-sided heart failure, the work load of this part of the heart needs to be increased in order to maintain the same extent of blood being supplied to the rest of the body, with an increased filling pressure.

A failing LV (with an increased pressure) leads to **backward failure**, which causes blood to stagnate in the pulmonary vessels where pressure increases. Since backward failure results in blood stagnating in the pulmonary vessels, causing pulmonary edema (congestion),

this could in turn affect the pulmonary perfusion distribution, as described in section 1.2.2 (lung zones).

1.4.2 Signs and symptoms

The typical signs of heart failure are dyspnea, fatigue and fluid retention. Fluid retention may lead to pulmonary crackles, elevated jugular venous pressure, peripheral edema and pulmonary congestion (edema).

1.4.3 Pulmonary edema

Pulmonary edema occurs when fluid is accumulated in the interstitial space or in the alveoli (Figure 1.6) and when the lymphatic drainage of this fluid is simultaneously insufficient or malfunctioning [24] [25] [26] [27] [28]. The edema will result in a larger distance for the gas exchange to occur between the alveoli and the capillaries. The gas exchange will then be reduced causing lower saturation. In the case of heart failure, pulmonary edema occurs due to that the LV is unable to efficiently pump the blood that is transported to it. Also, pulmonary edema occurs because of elevated left atrial pressure (LAP) [29]. This will result in stagnation of blood in the pulmonary vessels with increased blood volume in them and in the capillaries. As a result, the capillary hydrostatic pressure increases [25]. The accumulation of fluid is mainly located to the lower parts of the lungs due to gravity. The increased capillary pressure will result in increased filtration of fluid across the capillary walls to the interstitium. This will result in pulmonary edema if the accumulation of fluid is high, fluid can also enter the alveolar space.

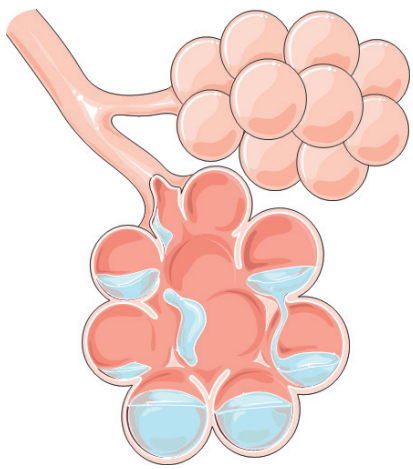

Figure 1.6: Image of the alveoli with accumulation of fluid.
Image modified and used with permission from Servier Medical Art - Creative Commons Attribution 3.0 Unported Licence.

1.4.4 Classification

Heart failure can be classified according to the New York Heart Association (NYHA) [1] based on patient's symptoms and ability to physical activity, see Table 1.1. However, the limitations of NYHA-classification shows aspects of subjectivity and patients experience their symptom's differently [30].

Table 1.1: Classification of heart failure according to New York Heart Association (NYHA).

NYHA
Class I: No limitation of physical activity. Ordinary physical activity does not cause undue breathlessness, fatigue, or palpitations.
Class II: Slight limitation of physical activity. Comfortable at rest, but ordinary physical activity results in undue breathlessness, fatigue, or palpitations.
Class III: Marked limitation of physical activity. Comfortable at rest, but less than ordinary physical activity results in undue breathlessness, fatigue, or palpitations.
Class IV: Unable to carry on any physical activity without discomfort. Symptoms at rest can be present. If any physical activity is undertaken, discomfort is increased.

1.4.5 Treatment

The treatment of patients with heart failure is based on their symptoms. The main purpose with treatments is to reduce mortality of the patients, improve quality of life and clinical status [1]. In systolic heart failure for example, the most important treatment is medical treatment. However, when optimal medical treatment is insufficient, implantable devices (with specific indications) are used. Implantable devices are cardiac resynchronization therapy (CRT) and implantable cardioverter defibrillator. Mechanical assist device such as intra-aortic balloon pump (for maintaining a good circulation), ventricular assist device, and mechanical circulatory support [31] are used as treatments when awaiting heart transplantation. Heart transplantation [1] is the final treatment alternative.

The focus in this thesis will be on treatment with CRT and heart transplantation.

CRT: is an invasive procedure where different leads of a device are placed in the LV. CRT is useful in selected patients with heart failure and need to fulfill the following criteria: EF below 35%, NYHA-classification III-IV, QRS duration >150 msc on electrocardiogram (ECG) and left bundle branch block [32] [33] [34]. In the case of left bundle branch block, there is irregular contractility of the septum as well as in the right and left ventricles. With this treatment, coordinated contraction of the right and left ventricles can be achieved. Patients will feel improvement in quality of life, symptoms and cardiac performance [35] [1]. Furthermore, the morbidity and mortality are also reduced [36]. However, there are patients (25–40%) that do not respond to this treatment [37].

Heart transplantation: is considered for patients with end-stage heart failure, where all available treatment options have failed. The patients are eligible for heart transplantation when they are in such a condition that they can manage the stresses post transplantation.

The focus in this thesis is investigating patients with heart failure before and after treatment with CRT and heart transplantation using the novel diagnostic method **Tomographic lung scintigraphy**, and using **Magnetic resonance imaging** (**MRI**) as a novel method to study the blood flow in the pulmonary circulation in patients with heart failure.

1.4.6 Diagnostic methods

There is not one single diagnostic method that can be used in the diagnosis of heart failure. There have to be several diagnostic methods that complement each other [1]. These include clinical assessment of symptoms and signs of heart failure. Before setting the diagnosis, a careful investigation of the medical history should be performed [1]. Furthermore, other diagnostic methods are, among others, echocardiography, chest X-ray and right-heart catheterization.

Echocardiography: is a non-invasive imaging method that investigates the systolic and diastolic function of the heart, volumes in the atria and ventricles, the valves and the thickness of the myocardial wall. It is useful in patients where heart failure is suspected [1]. Although echocardiography is widely available, cheap and has high temporal resolution, its limitations are that it could have a limited acoustic window [38] and is user dependent.

Chest X-ray: guidelines recommend to use chest x-ray as a non-invasive method in the diagnosis of pulmonary congestion in heart failure [1][39], especially in the acute setting of heart failure compared to the non-acute [40] [41]. From this examination, information can be obtained on heart size, pulmonary vessels and fluid in the lungs [39]. Furthermore, chest X-ray can be used to investigate differential diagnoses [1]. Heart failure diagnosis can be made if the heart is enlarged (cardiomegaly), if the pulmonary vessels are distended

and if fluid is present, more details are listed in section 4.4. This method has shown to have low sensitivity in the diagnosis of pulmonary congestion in heart failure [39][42][43]. This could be due to some compensatory mechanisms that compensate for the fluid shift in the lungs, covering the evidence of deranged hemodynamics [44]. In patients with suspected heart failure, chest X-ray is not useful [1]. Furthermore, patients with heart failure may present with normal chest X-ray even though having LV dysfunction [40] [41]. In addition, it can also be normal in patients (50-60%) who have pulmonary congestion and elevated pulmonary venous pressure [45][44]. In patients with acute decompensated heart failure, chest X-ray examination in supine position is inadequate [39].
Due to the low sensitivity of the recommended chest X-ray in the diagnosis of pulmonary congestion in heart failure, there is a need of other non-invasive diagnostic methods.

Right-heart catheterization: The indications of right-heart catheterization are [1]:

- To investigate patients with severe heart failure who will receive mechanical circulatory support
- To investigate patients who are under consideration for heart transplantation
- To evaluate patients with suspected pulmonary hypertension
- To investigate patients who still have symptoms although they are optimally treated with medications. This examination can be used in order to possibly adjust the treatment
- Is used on those with unstable hemodynamics

The hemodynamic variables that can be measured from this examination using a Swan Ganz catheter are CO, pulmonary artery pressure, pulmonary capillary resistance, the filling pressure in both right and left atrium as well as RV, HR and cardiac index. In addition, pulmonary artery wedge pressure (PAWP, which is an indirect measure of LAP) can be measured. The PAWP can be measured by inserting a catheter through the right internal jugular vein $\rightarrow$ right atrium $\rightarrow$ pulmonary artery $\rightarrow$ a smaller branch of the pulmonary artery until the catheter wedges. A balloon is then inflated and causes an obstruction of the blood in the smaller branch of the pulmonary artery.
A normal PAWP is 7 mmHg, and is regarded as elevated when it is >15 mmHg [46]. The catheter is linked to a computer where all these parameters are monitored during the procedure. Right-heart catheterization is regarded as the reference method in the diagnosis of pulmonary congestion. However, this method is invasive and could pose a risk for the patients [47].

1.5 Tomographic lung scintigraphy

Tomographic lung scintigraphy, also known as ventilation/perfusion single-photon emission computed tomography (V/P SPECT), is a non-invasive nuclear medicine examination. The examination enables a 3-dimensional imaging (visualization) of the distribution of the ventilation and perfusion in the lungs. The indications of a V/P SPECT examination are pulmonary embolism, chronic obstructive pulmonary disease, lung surgery, follow-up after treatment and pneumonia.

1.5.1 Image acquisition of V/P SPECT

In order to obtain images of the distribution of pulmonary ventilation and perfusion, specific radioactive aerosols and tracers are needed.

Ventilation: The method to quantify ventilation is by using aerosols. The definition of an aerosol is small particles that are suspended in gas. The etymology of the word aerosol is derived from the Greek and Latin and can be divided into two words: “aer” which means ”air” in Greek, and “solutio” which signifies ”solution” in Latin. When labelling a radioactive tracer to an aerosol it becomes a radioaerosol. A radioaerosol is small particles that can either be solid or liquid and the size of them is one of the factors that affect its deposition in the lungs [48] [49].
99mTechnetium (Tc)-Technegas is an aerosol that is used to study the ventilation in the lungs. It results in a high image quality, has large availability and also has lower costs compared to other radioactive gases [50]. Technegas has a small amount of focal depositions in the small and large airways, and is distributed homogeneously in the lungs [51]. Further on, the benefit of the use of 30 MBq of 99m-Tc Tehnegas in the ventilation study is also the low radiation effective dose of 0.45mSv. 99mTc-Technegas was first used for such purpose many years ago [52]. The aerosol Technegas contains ultrafine particles of solid graphite, labelled with the radioactive 99mTc that is distributed in the lungs proportionally to the ventilation. The ultrafine nanoparticles diffuse in the alveoli and have a 50% deposition fraction and are 0.02 micrometer in diameter [53]. The graphite nanoparticles are produced in a Technegas generator where all the particles are heated in a crucible with 99mTc in pure argon to 2550 degrees Celsius [54]. After the heating of the particles, they become small radioaerosols particles (with the size of 60nm-160nm) [55] and they have the same characteristics as radioactive gas [55] [56]. When inhaled, they adhere to the wall of the alveoli [52] [55] and have less impaction on conducting airway [55].

Perfusion: The method by which one can study the perfusion of the lungs is by using Macro-aggregated human albumin (MAA) labelled with 99mTc [57] [58]. 99mTc-MAA is produced by heating human serum albumin [58] and thereafter labeled with Tc. The size of the 99mTc-MAA particles is 15-100 µm and their size and shape is irregular. Their

main task is to create a microembolization at first passage through the lungs with a capillary blockage of the precapillary arterioles and pulmonary capillaries.
In order to obtain an accurate and even distribution of the 99mTc-MAA, a sufficient number of injected particles is needed. The injected number of particles need to be between 60 000-400 000 [57] [59]. Even though this sounds very much, this amount will only obstruct a small part of the pulmonary capillaries and arterioles. The regional distribution of the pulmonary perfusion is reflected by the distribution of the injected 99mTc-MAA particles. 99mTc-MAA is injected intravenously when the patient is in a supine position. The particles will be transported with the blood and reach the pulmonary arteries and capillaries through the right atrium and ventricle. After imaging has been performed, the particles will break down in the lungs and follow the blood from the lungs to the left atrium and ventricle and further to the systemic circulation.
The perfusion study (140 MBq 99mTc-MAA), with an effective dose of 1.64 mSv, is performed immediately after the ventilation study as a one-day protocol, with the patient in the same position. In order to overcome the activity from the ventilation dose of 30 MBq, the perfusion dose needs to be larger [60].
The half-time for 99mTc is six hours and the photopeak energy is 140keV.

Perfusion gradients: The calculation of the perfusion gradients was first developed by Jögi and co-workers in Lund, Sweden [61]. The perfusion gradients are automatically derived from the V/P SPECT images using a user-independent algorithm [61]. Perfusion gradients describe the change of the distribution of perfusion activity.
First, the algorithm receives input with all information from the perfusion images.
Second, the algorithm calculates the radioactivity (the amount of counts) in each voxel in the total lung volume (both lungs).
Third, for the algorithm to avoid artifacts and partial volume effect, about one centimetre (cm) of the outer borders of the lungs, large vessels and airways at the hili are automatically excluded.
Fourth, the values in each voxel are normalized to the maximum amount of activity in both lungs.
Fifth, the algorithm thereafter uses the total activity in all voxels of the lungs (from the fourth step) to perform a three-dimensional (3D) linear regression (line of best fit) for the distribution of total activity of the lungs. From the 3D linear regression, the algorithm extracts the slope in the posterior-anterior direction.
Sixth, the posterior-anterior slope from the 3D linear regression line describes the perfusion gradients. The unit of the perfusion gradients is percent counts per cm, which is the change in relation to the normalized distribution of the perfusion activity per cm lung.

The perfusion gradients are a measure of the distribution of pulmonary perfusion.

Images of the regional pulmonary ventilation and perfusion are taken using a gamma cam-

era.

Gamma camera: A gamma camera consists of collimators, sodium iodide crystal (scintillator) and many photomultiplier tubes. Gamma cameras have different numbers of heads (detectors). The most common is dual-heads, and the gamma cameras that has been used in this thesis have dual-heads with two detectors. The emitted photons hit the crystal and are transformed thereafter to visible light. The light is later detected by the photomultiplier tubes and the energy from the emitted photons (from the patient) is registered as an electrical signal by the photomultiplier tubes. Their task is, except to spread the light from the emitted photons through the crystal, also to choose where the photons hit the crystal. The light is thereafter localized by a computer. The use of collimators with many parallel holes in the gamma cameras enables good resolution of the images and that emitting photons hit the crystal perpendicularly, which generates an image. On the other hand, some of the emitted photons will not hit the crystal because they are emitted in an oblique way.
For the V/P SPECT examination, static acquisition is acquired, and the two detectors rotate around the patient. Three different electrical signals (x, y and z pulses) are obtained from the detectors to produce the images. These electrical signals reflect how much energy the photons consist of and where in the crystal the photons are absorbed. The distribution of the radioactive tracers in the images is then reconstructed using a computer to obtain images with different slices (planes); transversal, sagittal and coronal.
After acquiring the V/P SPECT images, the images are reconstructed using iterative reconstruction. This method is based on an algorithm where a continuous adjustment of an image assumption is made until the reconstruction reach an image with the true values (true distribution of the radioactive isotope) in the examined plane. Accumulation of the radio active isotope in the lungs (also named hot spot), could arise and is reduced during the reconstruction of the ventilation and perfusion images. Next step in the reconstruction process is to subtract the ventilation from the perfusion image. The final step is normalization of the ventilation and perfusion images, resulting in V/P quotient [60].

1.5.2 Interpretation of V/P SPECT image

Ventilation images: in a patient with heart failure with pulmonary congestion, the ventilation is affected, but not as the perfusion images.

Perfusion images and perfusion gradients: In a normal healthy person, the distribution of pulmonary perfusion is located in the lower parts of the lungs (in the base when standing, and dorsal/posterior when lying in supine position). The alveoli are more open in the lower parts of the lungs. In a patient with heart failure and pulmonary congestion and increased LAP, the fluid is accumulated in the interstitum and affected by the gravity (pulmonary edema). This will in turn affect the capillaries and small vessels (they become compressed and less distensible) in the lower parts of the lungs and a decreased gas exchange. A redis-

tribution of pulmonary perfusion to higher located parts of the lungs (apex when standing, anterior when lying in supine position) will then occur since the vessels are closed in the lower parts of the lungs. In West zone III [8] (which is located in the lower part of lung, base) the capillaries are open and there is blood flow through them. When the redistribution of pulmonary perfusion occurs, West zone III is relocated to higher located parts of the lungs, see figure 1.4 [8]. The redistribution of pulmonary perfusion has previously been seen and quantified using perfusion gradients in patients with heart failure [61].

The redistribution of pulmonary perfusion to upper or anterior parts of the lungs causes the perfusion gradients to become positive (> 0%-counts/cm, positive slope of the perfusion gradients). When the distribution of the pulmonary perfusion is normal and therefore located in the lower (base, dorsal, posterior, depending on patient position) parts of the lungs, this yields a negative value of the perfusion gradients (< 0%-counts/cm, negative slope of the perfusion gradients). The redistribution of pulmonary perfusion in the previous study was associated with positive perfusion gradients in the posterior-anterior direction [61].

V/P quotient images are when the ventilation and perfusion images are fused together to present a quotient between the two. In a patient with heart failure and pulmonary congestion, the V/P quotient image will be mismatched, but not in a segmental way as seen in patients with pulmonary embolism.

1.6 MRI

MRI is a non-invasive imaging method.
Hydrogen (H+) is an element which is an essential part of many different chemical compounds in the human body such as water, fat, and proteins. A hydrogen atom has one proton with positive charge and is associated with one electron with negative charge. Protons have a property called spin which gives rise to a magnetic moment. These magnetic moments are normally oriented randomly. An magnetic resonance (MR)-scanner has a strong magnetic field called B_0. The strength of the magnetic field is usually 1.5 Tesla (T), but it could also be 3 or 7 T. When the patient is placed in the MR-scanner, the patient's hydrogen atoms are affected by the external magnetic field. The magnetic moments of the protons are then aligned such that the net magnetic moment from all protons is aligned parallel to the external magnetic field. In addition to aligning with the external magnetic field, protons also precess around it. The precession frequency can be calculated using the following equation, called Larmor equation [62]:

$$\omega_0 = \gamma * B_0 \tag{1.4}$$

Where ω_0 is the precession frequency in Hz, γ is the gyromagnetic ratio and B_0 is the strength of the external magnetic field given in Tesla (T). ω_0 is proportional to how strong

B_0 is. To create an MR signal, the scanner sends a specific radio frequency (RF) pulse to the patient. This pulse is an electromagnetic wave. Its main function is to disrupt the alignment of the protons along the external magnetic field. It needs to be an RF pulse on resonance with the proton precession, i.e. it needs to be an RF pulse with frequency ω_0.

Gradient system. There are three gradient coils in the MR-scanner. These coils are used to identify the location of the MR signal. When a gradient is activated a magnetic field is created which varies in strength along either the X, Y or Z direction in space. To create an image, the MR signal has to be localized to a specific position. This can be performed by creating variations in the magnetic field with the gradient coils. The Larmor frequency of the protons in the body will now vary depending on its location in space. The RF pulses of an MR-scanner can be adjusted to only contain a narrow band of frequencies. When such an RF pulse is applied at the same time as one of the gradient coils is activated, only protons within a thin slice perpendicular to the gradient direction will be affected by the RF pulse. The resulting MR signal will therefore only originate from this slice. This is called slice selection and is used to localize the MR signal along one direction. In order to localize the MR signal along the two remaining orthogonal directions the gradient coils are used to encode a phase and frequency variation of the protons along two perpendicular directions parallel to the slice. Phase encoding is performed by activating the gradient coils before receiving the MR signal and frequency encoding is performed by activating the gradient coils at the same time as the MR signal is received. The collected phase- and frequency encoded MR signal can be sorted in a two-dimensional (2D) coordinate system called K-space. K-space is a coordinate system that stores the spatial frequency of the MR signal. One voxel in K-space represents every voxel in the image and vice versa. In the center of K-space, are the low spatial frequencies, which represents the general shape of the image. For example, if only the central part of K-space is reconstructed, the heart can be seen but it will be blurry. The outer part of K-space represents the high spatial frequencies, which are the edges and the details. This information is needed to see valves of the heart for example. The mathematical Fourier transform is needed to transform K-space into an MR image.

1.6.1 Cine images

The motion of the entire heart can be obtained using MRI images, called cine images. This can be done by synchronizing the MR acquisition to the patient's ECG-signal. The acquisition takes place during end-expiratory breath-holds in order to avoid image artifacts. Images of the heart is usually taken in long axis views and in short axis views that covers the LV from apex to atrium. Manual delineation of the EDV and ESV can be done during end-systole (ES) and end-diastole (ED) as well as calculating SV and EF [63].

1.6.2 Phase contrast MRI

Phase contrast MRI is a method used to measure flow. Flow measurements using MRI is a non-invasive method that has good accuracy [64][65][66][67]. Two different images are acquired: 1) anatomical or magnitude image (to be able to see and define the contour of the vessel), and 2) the phase image (to obtain the flow velocity). The vessel of interest is examined in cross-section, having a defined image plane perpendicular to the vessel. By applying a bipolar gradient pulse to the vessel, the moving blood particles obtain a phase shift which depends on their velocity and magnetic field imperfections. By taking the phase difference between two repeated measurements with opposite bipolar gradient polarity the signal component from magnetic field imperfections can be removed and the remaining phase signal is proportional to the flow velocity. In MRI, the velocity encoding gradient (VENC) is a parameter that controls the maximum velocity that can be measured in a phase contrast measurement. The VENC should be chosen and set slightly above the maximum velocity of the vessel of interest. If the VENC is set too low, this will result in inability to detect fast flows. If the velocity in the vessel supersedes the VENC the measured velocity will appear to have the opposite direction from the true flow. This is called velocity aliasing. Too high VENC on the other hand cannot identify small flow velocities, will result in poor image quality and is unable to visualize vessels that have inert flow. The flow images are obtained during the whole cardiac cycle using cine imaging (see section 1.6.1). In order to obtain the flow during one cardiac cycle, delineations of the vessel can be performed by drawing a region of interest around the lumen of the vessel.

Chapter 2

Rationale

The pulmonary perfusion, which is affected in patients with heart failure due to pulmonary congestion, can be non-invasively assessed according to guidelines using chest X-ray, and invasively by right-heart catheterization. Studies have shown that chest X-ray is limited, and catheterization is invasive [39][42][43][47]. Hence, there is a need for a non-invasive method in the diagnosis of pulmonary congestion in heart failure. In 2008, it was shown that the non-invasive method V/P SPECT can be used in the diagnosis of pulmonary congestion in heart failure to quantify pulmonary perfusion distribution [61]. However, this method required validation. The project in this thesis was started in 2013, where V/P SPECT was aimed to be validated with right-heart catheterization and follow-up treatment effect.
Also, investigating the new method using MRI and its role in heart failure is important, since it has never been performed previously.

The studies in this thesis are needed in order to 1) avoid invasive catheterizations in selected cases, 2) aid in treatment decision, 3) to follow-up treatment effect non-invasively, and 4) to investigate if a new measure using MRI can complement other examinations in heart failure.

No such studies have been made previously, and the hope is that this thesis and the studies will aid in the understanding of the pathophysiology of pulmonary congestion in heart failure. Furthermore, this thesis also aims to develop non-invasive assessment and quantification of pulmonary blood flow in heart failure.

Chapter 3

Aims

The general aim of this doctoral thesis was to develop and validate new non-invasive methods to diagnose, quantify and follow-up pulmonary congestion in heart failure, and to study the variation of the blood flow in the pulmonary circulation.

The specific aims of each paper was to:

Paper I: evaluate the potential of V/P SPECT as a non-invasive method to assess and quantify pulmonary congestion in patients with severe heart failure who were under consideration for heart transplantation and used right-heart catheterization as reference method. Furthermore, the performance of V/P SPECT compared with chest X-ray was investigated in the clinical setting.

Paper II: investigate if V/P SPECT can be used to assess treatment effect after heart transplantation using invasive right-heart catheterization as the reference method.

Paper III: assess if changes in perfusion gradients from V/P SPECT are associated with improvement in heart failure symptoms after CRT. In addition, to evaluate if perfusion gradients from V/P SPECT correlate to currently used methods in the follow-up of patients with heart failure after receiving CRT.

Paper IV: evaluate whether the pulmonary blood volume variation (PBVV) differs in patients with heart failure compared with healthy controls and investigate the mechanisms behind the PBVV.

Chapter 4

Material and Methods

4.1 Study populations

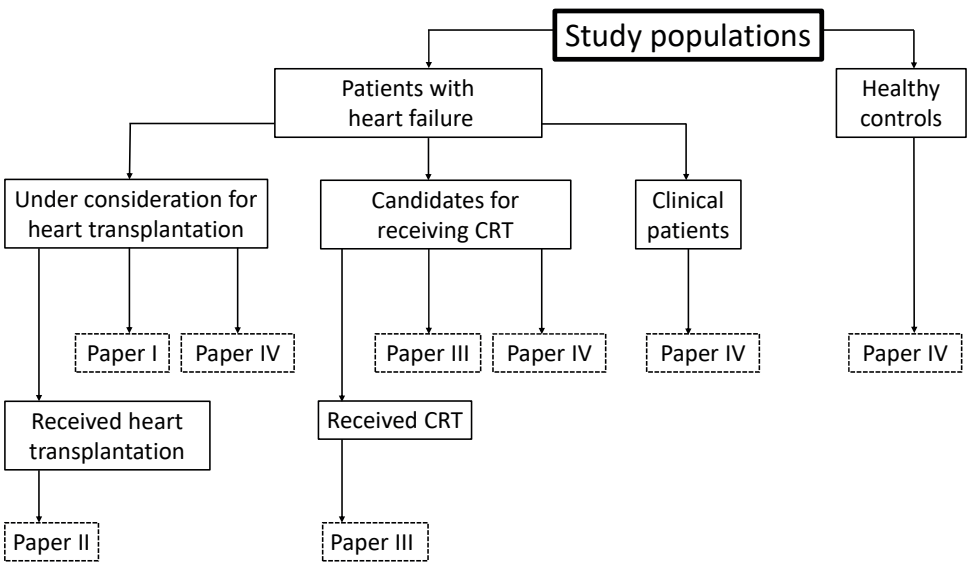

Figure 4.1: A summary of all the study populations included in the four papers in this thesis.

An overview of the included study populations in this thesis is shown in Figure 4.1. Paper I and IV included patients with heart failure who were under consideration for heart transplantation. Paper II included patients with heart failure who received treatment with

heart transplantation and paper III included patients before and after receiving CRT. Paper IV included patients who were candidates for receiving CRT, clinical patients with heart failure and healthy controls. All patients and five of the healthy controls were prospectively included. The patients performed all examinations at Skåne University Hospital in Lund, Sweden. All patients and healthy controls gave their informed consent before participating in the studies and the ethical board at Lund University in Sweden approved the study. The V/P SPECT examination was the only examination that was performed as part of the project. The other examinations were performed with clinical indication. Exclusion criteria were pregnant women, severe kidney failure with glomerular filtration rate <30ml/min and patients <40 years.

Paper I

Paper I included 46 patients with severe heart failure who were under consideration for heart transplantation between the years 2013-2017. The patients underwent V/P SPECT, invasive right-heart catheterization and chest X-ray.

Paper II

Twenty-three patients were included in paper II after receiving treatment with heart transplantation. Seventeen of these patients were also included in Paper I, and the rest (6/23) were included after the publication of paper I and were therefore new patients. The patients underwent V/P SPECT and invasive right-heart catheterization between the years 2013 and 2019.

Paper III

Paper III consisted of 19 patients with heart failure who were candidates for receiving CRT. The patients underwent V/P SPECT and echocardiography before and after receiving CRT between 2013-2017. Paper III is a sub study of a larger clinical trial study (CRT clinic). Of the patients included in paper III, seven were randomized to extended diagnostic imaging before CRT and 12 patients were controls that underwent standard imaging assessment pre CRT in the main study. The number of left ventricular end-systolic volume (LVESV) responders in the two groups were not different (three and four, respectively). As the original CRT clinic study was negative the patients in the current sub study were considered as one group.

Paper IV

Paper IV included 46 patients with heart failure during the period 2014-2017. These patients were under consideration for heart transplantation (n=4 from paper I, n=1 from paper I and II after heart transplantation), candidates for receiving CRT (n=15 from paper III, and n=3 that were not included in paper III), and clinical patients (n=23). In addition, 10 healthy controls were also included. The patients underwent MRI examination and echocardiography.

4.2 V/P SPECT and perfusion gradients

The same procedure and image acquisition of the V/P SPECT examination was performed in Paper I-III, where the distribution of pulmonary ventilation and perfusion was assessed. The Gamma cameras that were used for the examinations were either Discovery NM/CT 670 or Discovery NM 630 (GE healthcare Sverige AB, Danderyd, Sweden), with dual-heads. The examination was performed as a one-day protocol and the patients were in supine position when investigated. The examination was initiated with the ventilation study, where the patients inhaled 99mTc-Technegas (Cyclomedica Ltd, Dublin, Ireland) until 30 MBq reached the lungs. The examination proceeded with the investigation of perfusion, where the patients received an intravenous injection of 140 MBq 99mTc-MAA albumin (TechneScan LyoMAA; Mallinckrodt Medical BV, Petten, Netherlands). In order to be able to acquire the ventilation and perfusion images and compare them with each other, the patient remained in the same supine position in the perfusion study as for the ventilation study. The collimator that was used was an extended low-energy general purpose and the images were acquired in a total of 120 projections for both the ventilation and perfusion studies, respectively.
The acquisition time for the ventilation was 10 seconds/projection, resulting in 20 minutes. The time for the acquisition of the perfusion was 5 seconds/projection, yielding 10 minutes.

Visual (qualitative assessment). The V/P SPECT images were qualitatively assessed in Paper I. The distribution/uptake of the radioactive isotope in the lungs was assessed. The images were assessed with regard to pulmonary congestion. A redistribution of pulmonary perfusion from posterior to anterior parts of the lungs was regarded as a sign of pulmonary congestion. The ventilation images were also assessed, despite that it is usually not affected to the same degree as the perfusion SPECT images.

Perfusion gradients. The perfusion gradients were automatically derived from the perfusion SPECT images using the previously described algorithm [61]. Perfusion gradients in the posterior-anterior direction were used in these studies. Positive perfusion gradients indicate redistribution of pulmonary perfusion to higher located parts of the lungs and therefore sign of pulmonary congestion [61]. Negative perfusion gradients on the other

hand, indicate normal pulmonary perfusion distribution.

4.3 Right-heart catheterization

The right-heart catheterization examination in Paper I and II was performed at the Haemodynamic Lab, Skåne University Hospital in Lund, Sweden. The purpose of this examination was to measure/monitor haemodynamic measurements of the heart. This was accomplished using a Swan-Ganz catheter (Edwards Lifesciences, Irvine, CA, USA) inserted via the right jugular vein. The following parameters were measured/monitored:
-mean PAWP,
-mean arterial pressure,
-mean right atrial pressure,
-mean and diastolic pulmonary artery pressure (mPAP, dPAP).

In addition, the following parameters were calculated:
-SV= CO/HR,
-Cardiac index = CO/body surface area,
-Transpulmonary gradient (TPG) = mPAP x PAWP,
-pulmonary vascular resistance = TPG/CO,
-diastolic pulmonary vascular pressure gradient = dPAP – PAWP.

An ECG was recorded during the examination, in order to register the HR
PAWP with >15mmHg was used as a cut-off value for pulmonary congestion [46].

4.4 Chest X-ray

The chest X-ray examination was performed at the Radiology department, Skåne University Hospital in Lund, Sweden and used in Paper I. During the examination, the patients were in upright position. The X-ray unit that was used was digital with the following parameters: 140kV and 200mA. The images of the lungs were taken in posterior to anterior direction. The chest X-ray images were assessed (qualitatively) for signs of pulmonary congestion with the following criteria:
-pleural effusion,
-peribronchial cuffing,
-upper lobe venous diversion,
-increased cardiothoracic ratio,
-thickening of interlobar fissures,
-Kerley B lines.

4.5 CRT

Paper III included patients who were candidates for receiving CRT. Paper III is a sub study of a larger clinical trial study with 102 patients, named CRT clinic, (ClinicalTrials.gov Identifier: NCT01426321, CRT clinic).
The main methodology of the original study has been published [68]. The patients in the original CRT clinic study were randomized either after intervention (which is extended examinations using MRI, computed tomography and echocardiography) or according to clinical routine. For the intervention group, the physician who placed the CRT electrodes could use the results from the examinations.

4.5.1 Endpoints

The endpoints and criteria used to categorize patients as responders or non-responders to CRT were as follows: quality of life scoring system for heart failure (Minnesota living with heart failure (MLWHF)) (with $\geq$ 10% relative reduction) [69] NYHA-classification (with $\geq$ 1 class improvement) [70] [71]. From echocardiography, left ventricular ejection fraction (LVEF) (with absolute increase of $\geq$ 10%) and LVESV (with relative reduction of $\geq$ 15%) [72] were used as endpoints.

4.6 Echocardiography

Transthoracic echocardiography was used in paper III and IV and performed in line with guidelines [73]. The ultrasound apparatus for paper III was a Vivid 7, GE Medical, Horten, Norway. The systems used in paper IV were Vivid E9/Vivid 7, GE Medical, Horten, Norway or iE33/Epic/CX50, Philips Healthcare, Eindhoven, Netherlands.
In paper III, the 2- and 4-chamber views were used to calculate (manually) the endocardial contours. The biplane simpson method was then used to calculate the LV EDV and ESV as well as the EF. The echocardiographer performing examinations had more than 10 years experience.

4.7 MRI

Two different MRI scanners (1.5 Tesla) were used in paper IV. For subjects included 2013-2014, a Philips scanner (Achieva, Philips Medical Systems, Best, the Netherlands) was used. Furthermore, a Siemens scanner (Aera, Erlangen, Germany) was used for subjects included in 2015-2017.
In order to study cardiac function, cine short and long axis images (of the heart) were acquired using a standard sequence named balanced steady-state free precision. Also, the examinations were ECG-triggered for all subjects in endexpiratory breath-hold. The function and volumes of the LV and RV were manually calculated (in planimetry) in the cine

short axis images [74]. The volumes and function that were measured were EDV and ESV. The planimetric SV was then calculated as EDV-ESV and EF as SV/EDV times 100. Here follows the specific MR parameters for the cine images:
MR-scanner Philips Achieva= Slice thickness: 8 mm, Slice gap: 0 mm, Repetition time (TR): 2.6 ms, Echo time (TE): 1.5 ms, Flip angle: 60°, Pixel size (reconstructed): 1.5 x 1.5 mm.
MR-scanner Siemens Aera= Slice thickness: 6 mm, Slice gap: 2 mm, TR: 2.6 ms, TE: 1.2 ms, Flip angle: 59°, Pixel size (reconstructed): 1.0 x 1.0 mm.

In paper IV, the flows in the main pulmonary artery and pulmonary veins were measured using a 2D flow sequence, nonsegmented phase contrast velocity-encoded gradient sequence. The flow acquisition was performed with imaging slice positioned perpendicular to the vessel and with retrospective ECG-triggering. Several cardiac cycles were averaged to create a flow curve covering one cardiac cycle.
The flow in the main pulmonary artery was acquired during free-breathing for all subjects, which is approximately 170 cardiac cycles. The flow in the pulmonary vein was acquired during either free-breathing (in 16 patients) and consisted of approximately 140 cardiac cycles or during breath-hold (at end-expiratory) in 21 patients and consisted of approximately 20 cardiac cycles in total. For the healthy controls, the flow in the main pulmonary artery and pulmonary veins were acquired during free-breathing. Here follows the specific MR parameters for the flow images:
MR-scanner Philips Achieva, free-breathing images= Slice thickness: 5 mm, Reconstructed frames per cardiac cycle: 35, TR: 8.7 ms, TE: 6.4 ms, Flip angle: 15°, Pixel size: 1.2 x 1.2 mm, VENC (arterial flow): 200 cm/s, VENC (venous flow): 80 cm/s.
MR-scanner Siemens Aera, free-breathing images= Slice thickness: 5 mm, Reconstructed frames per cardiac cycle: 30, TR: 9.8 ms, TE: 2.7 ms, Flip angle: 20°, Pixel size: 1.5 x 1.5 mm, VENC (arterial flow): 200 cm/s, VENC (venous flow): 80 cm/s.
The MR parameters are the same for the breath-hold images as for the free-breathing images. However, only the following differs= TR: 39.4 ms, TE: 2.7 ms, Pixel size: 1.8 x 1.8 mm.

4.8 PBVV

The PBVV in paper IV describes the change of maximum variation of the blood volume in the pulmonary circulation during one cardiac cycle [75]. The PBVV can be measured by using blood flow measurements from the main pulmonary artery, which is the inflow of blood to the pulmonary circulation, and blood flow measurements from the pulmonary vein, which is the outflow of the blood from the pulmonary circulation. These flows are measured using MRI [75]. Figure 4.2 presents a schematic image of the PBVV and Figure 4.3 presents a detailed description of the calculation of PBVV.

PBVV has been investigated in pigs and showed to be decreased following acute myocardial infarction [76]. PBVV has later been investigated in patients with systemic sclerosis where it was unchanged compared to healthy controls [77]. However, PBVV has never been investigated in patients with heart failure.

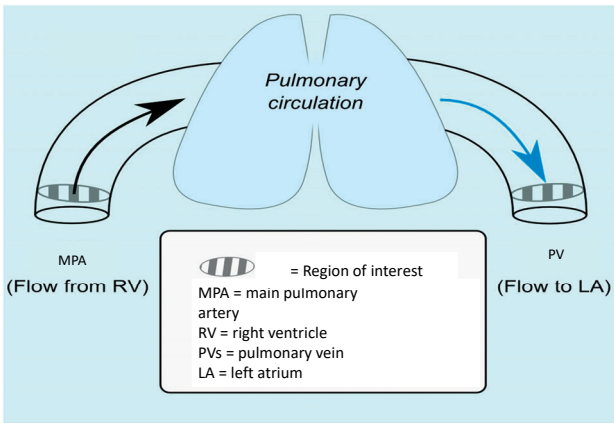

Figure 4.2: Schematic illustration of the pulmonary blood volume variation (PBVV) using magnetic resonance imaging. The flow in the main pulmonary artery (entering the lungs through the pulmonary circulation, black arrow) and in the pulmonary vein (leaving the lungs, blue arrow) are measured with their corresponding area with region of interest. These two vessels are shown in the figure as one vessel.
Adapted and edited with permission from Mikael Kanski [10].

First, the flow in the main pulmonary artery (inflow, shown in black) was measured during systole (Figure 4.3 (1)). Note that the vast majority of the SV is produced during systole.
Second, the flow in all pulmonary veins (outflow, shown in blue) was measured (4.3 (2)). Panel 3 in Figure 4.3 shows the measurement in one pulmonary vein (presented in blue and the solid line). The dashed blue line represents the scaled flow to match the flow in the main pulmonary artery.
Third, Figure 4.3 (4) shows the difference between the blood flow of the inflow (arterial) and outflow (venous). Note that there is a positive blood flow during systole and negative blood flow during diastole. The integral of this curve was calculated over time.
Fourth, the graph that was obtained in Figure 4.3 (4) presents the cumulative blood volume in the pulmonary circulation (4.3 (5)). The definition of PBVV was the difference between the maximum and the minimum of the cumulative volume variation over the cardiac cycle (represented by the double-headed arrow).
The average of the pulmonary vein and pulmonary artery time-step was used for calculating

the cumulative blood volume, since there were 35 time frames over the cardiac cycle and the HR might vary during the examination.

Lastly, the PBVV was indexed to the effective SV in the main pulmonary artery, in order to account for any variations in the ejected SV from the RV, $PBVV_{SV}$. The value was presented as a percentage. The SV is the area under the curve of the flow profile in the main pulmonary artery.

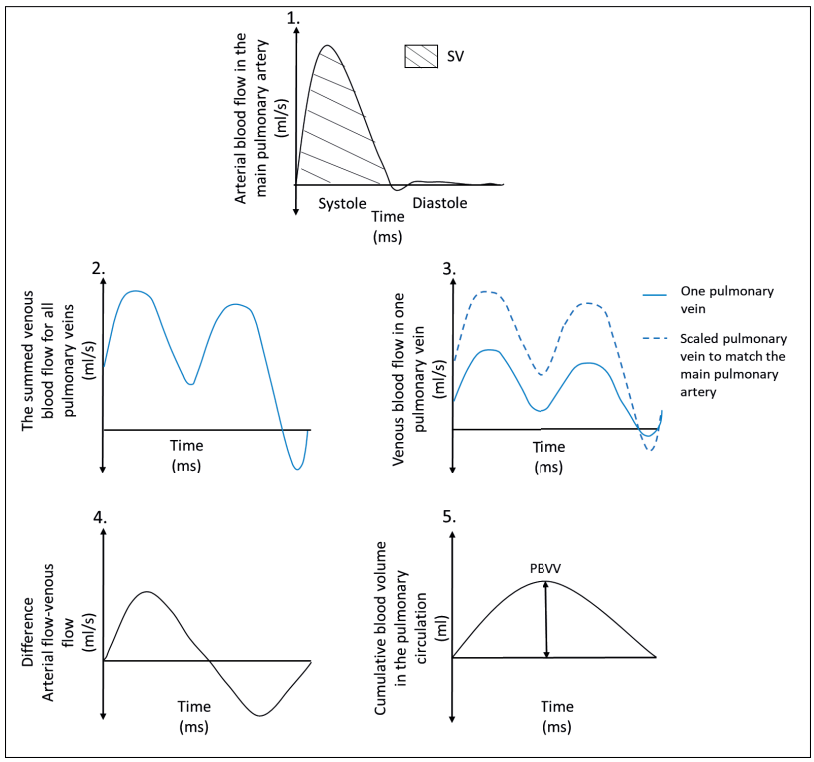

Figure 4.3: A schematic figure of the different steps in the calculation of the pulmonary blood volume variation (PBVV) indexed to stroke volume (SV) using the blood flow measurements in the main pulmonary artery and in the pulmonary vein, measured from magnetic resonance imaging.

Flow measurements. A region of interest was manually delineated around the lumen of the investigated vessels in order to obtain the flow in them. The blood flows were calculated in the software Segment (see below under the section "Image analysis") using the following formula: vessel area (cm^2) times mean through-plane velocity (cm/s) = cm^3/s = mL/s. The vessels of interest were the main pulmonary artery and pulmonary veins, see Figure 4.4.

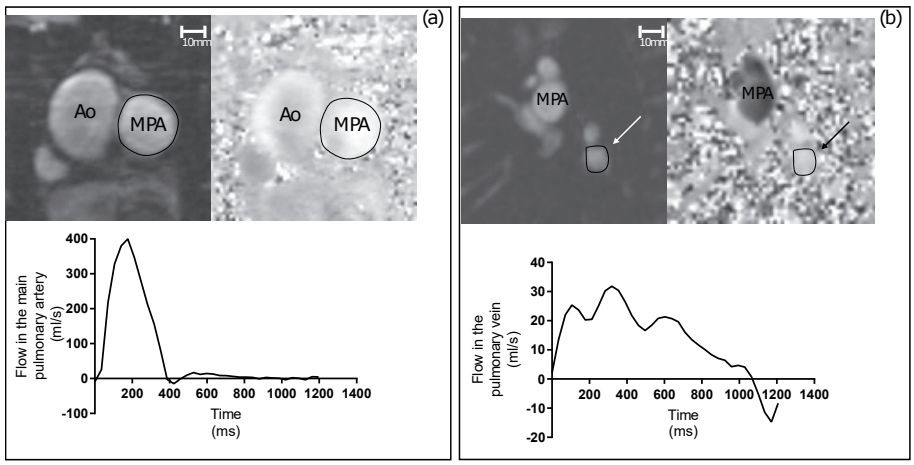

Figure 4.4: Magnetic resonance images (magnitude and phase) in a healthy control.
(a) Image of the main pulmonary artery (MPA) and the corresponding flow curve. AO: aorta.
(b) Image of the pulmonary vein and the corresponding flow curve. The white and black arrows points toward the pulmonary vein.
A region of interest (in black) was manually delineated around the vessels.
Dimensional bars: 1 cm = 10 mm.

An internal validation was performed in a subset of the patients and healthy controls, in order to investigate if there were any differences between breath-hold and free-breathing sequences when calculating the PBVV. It is also known that patients usually have difficulties in holding their breath, resulting in respiratory motion artefacts, despite the fact that a breath-hold sequence is faster than a free-breathing one. The internal validation was made in nine patients and five healthy controls where the two sequences were acquired in all of the patients.

In order to investigate if it is possible to use the measurement of one pulmonary vein, instead of the measurements of all pulmonary veins, in the calculation of PBVV, a second validation was performed. The validation was made in nine healthy controls and four patients with heart failure. In addition, an intra- and interobserver variability were performed in 10 patients with heart failure by two observers for the flow measurements of the main pulmonary artery and pulmonary vein, as well as for the calculation of PBVV and $PBVV_{SV}$.

4.8.1 Other parameters investigated in paper IV

The **AV-plane displacement (AVPD)** of the LV and RV was calculated in ES and ED. This was calculated by manually placing input points in 2-, 3- and 4-chamber long-axis cine MRI images of the LV and RV.
The movement of the LV AV-plane in the apical to basal direction is the definition of **LVAVPD** [78] [79] [80].

Systolic volume was calculated in the flow measurement of the pulmonary vein. It was defined as the cumulative volume of the venous flow during systole.

Phase shift: in order to study the phase shift between the in- and outflow, the cumulative blood volume values were interpolated with a cubic spline using Matlab version R2016b (Math-Works, Natick, MA). A smoothed curve was then obtained and the peak value of this curve was used.
The phase shift between the in- and outflow (main pulmonary artery and pulmonary vein) can also be described as the timepoint for when the maximum pulmonary blood volume occurs, as a percentage of the cardiac cycle and shown in Figure 4.5. The Figure presents how the flow curve in the pulmonary vein and the PBVV curve are shifted when the $PBVV_{SV}$ is increased, compared to normal $PBVV_{SV}$.

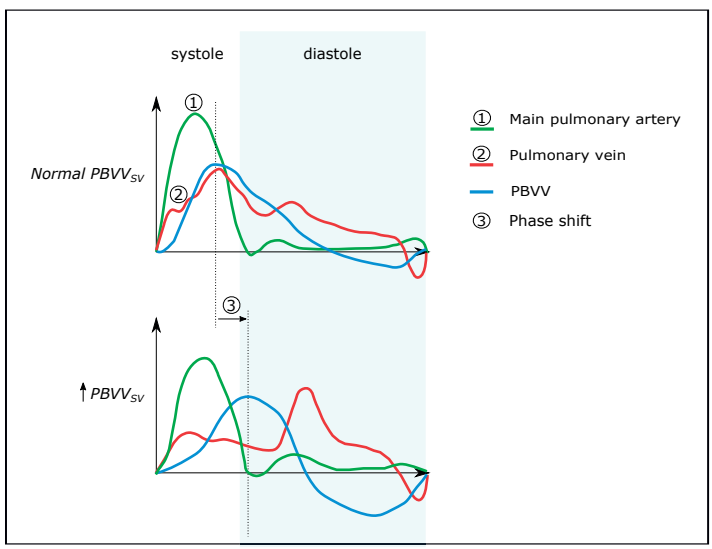

Figure 4.5: Flow curves of the main pulmonary artery (green), pulmonary vein (red) and pulmonary blood volume (PBVV, blue) during normal and increased PBVV indexed to SV ($PBVV_{SV}$). Note how the curve of the pulmonary vein and PBVV are shifted to the right during increased $PBVV_{SV}$. During normal conditions there are more blood during systole in the pulmonary vein compared to diastole. However, during increased $PBVV_{SV}$ there is less blood during systole and more during diastole, resulting in a phase shift.

Area variation of the large vessels: the relation between the area variation of the main pulmonary artery and the pulmonary vein with respect to PBVV in patients with heart failure and healthy controls were investigated. This is to ascertain if the variation in the bigger vessels affects the PBVV. The difference between the maximum and the minimum of the vessel area was used to define the are variation of each vessel in patients with heart failure and healthy controls.

4.9 Image analysis

V/P SPECT

Oasis Pulmogam software (Segami corp., Columbia, MD, USA) was used to visually evaluate the V/P SPECT images. Ordered Subset Expectation Maximization was used to reconstruct (iteratively) the images.

Echocardiography

The echocardiographic images were analyzed and reviewed using a workstation by GE Medical, Horten, Norway, named Echopac BT12 for paper III and IV.

MRI

The software Segment version 2.2 R6901 (Medviso, Lund, Sweden) [81], which is a freely available software, was used to assess and analyze the MRI images.

4.10 Statistical analysis

The two different programs that were used for statistical analysis were SPSS statistics versions 23.0 and 25.0 (IBM Corp, Armonk, NY, USA) and GraphPad Prism versions 6.0, 7.04 and 8.4.2 (GraphPad Software, La Jolla, CA, USA)
Histograms were used to test whether the data was normally distributed or not. The data was therefore expressed as mean $\pm$ standard deviation (if normally distributed) or median and interquartile range range [IQR] (if not normally distributed). It is stated in each paper how the data is presented. A p-value of <0.05 was considered statistically significant in all papers.
In paper I, independent t-test was used to investigate the difference between increased/normal PAWP and presence/absence of pulmonary congestion in V/P SPECT and chest X-ray. Furthermore, intra- and interindividual visual assessment was performed for comparison between V/P SPECT and clinical reports of V/P SPECT and chest X-ray and by expert readers (for visual assessment of the V/P SPECT images), using Cohen's kappa test.
The sensitivity, specificity, positive predictive value (PPV), negative predictive value (NPV)

and accuracy were also calculated.

In paper II, paired t-test was used in order to investigate the difference in perfusion gradients before and after heart transplantation. Furthermore, it was also used to study the PAWP before and after heart transplantation. To investigate the relationship between perfusion gradients and PAWP (before and after heart transplantation), Pearson correlation was used.

In paper III, to investigate if there is a difference in LVESV and perfusion gradients before and after CRT, Wilcoxon signed test was used. Fisher's exakt test was used when investigating the difference between improved/non-improved perfusion gradients vs improvement in NYHA-classification, MLWHF quality of life scoring system, LVESV and EF. Fisher's exact test was also used to investigate the difference between improved/non-improved LVESV vs NYHA-classification, MLWHF quality of life scoring system, LVEF and perfusion gradients.

In paper IV, Mann-Whitney's test was used to study quantitative, not normally distributed independent data; comparison between patients with heart failure and healthy controls regarding PBVV and $PBVV_{SV}$ results. This test was also used to investigate the relationship between $PBVV_{SV}$ and vessel area variation. The regression analysis in paper IV was performed using Spearman correlation. Furthermore, Wilcoxon signed test was used to:

1. compare the breath-hold sequence images with the ones of free-breathing in healthy controls and patients with heart failure.
2. compare the PBVV that was calculated using one pulmonary vein and all pulmonary veins.

The diagnostic accuracy between the $PBVV_{SV}$ and the phase shift between the in- and outflow was also investigated using the cut-off value calculated by the averages $\pm$ 2 SD of a normal $PBVV_{SV}$.

Multiple regression analysis was used in order to study which variables explain the variation of $PBVV_{SV}$ in patients with heart failure. First, the correlation between all variables with $PBVV_{SV}$ was studied (univariate regression analysis). The variables that were included in the multiple regression analysis model were those with p-value < 0.10 from the univariate analysis. It was decided to exclude the higher p-value if two or more variables showed colinearity between each other. Colinearity was present when there was a statistically significant correlation between two or more dependent variables.

Chapter 5

Results and comments

The major results of the four papers are presented in this chapter. More details can be found in the respective papers at the end of the thesis.

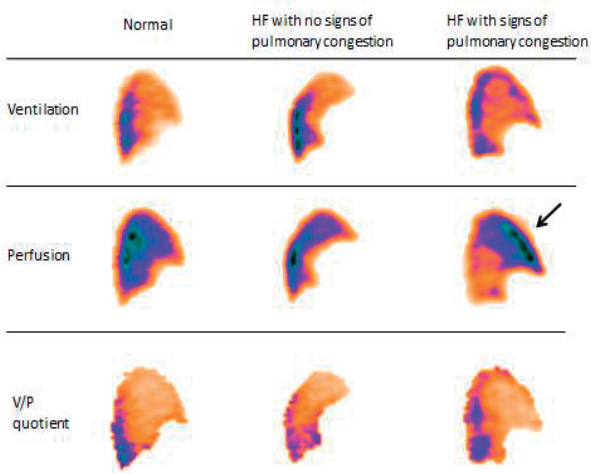

Figure 5.1: Ventilation/perfusion single-photon emission computed tomography (V/P SPECT) images including the ventilation, perfusion and V/P quotient of a normal patient, a patient with heart failure (HF) with no signs of pulmonary congestion and a patient with HF with signs of pulmonary congestion. The black arrow points towards the redistribution of pulmonary perfusion in the patient with signs of pulmonary congestion, which is not present in the normal person and in the patient with no signs of pulmonary congestion.

5.1 Paper I: Diagnosis and quantification of heart failure using V/P SPECT and validated using right-heart catheterization

V/P SPECT image

Figure 5.1 shows V/P SPECT images of a normal patient and patients with heart failure with and without signs of pulmonary congestion. The patient who had heart failure with signs of pulmonary congestion showed a redistribution of pulmonary perfusion.

Comparison between PAWP and signs of pulmonary congestion on V/P SPECT and chest X-ray

This is the first study that validates and compares perfusion gradients with PAWP. The comparison between PAWP and assessment of V/P SPECT images, with regard to presence/absence of pulmonary congestion, performed by expert reader 1 and 2 is shown in Figure 5.2 A and B. There was a small overlap and a significant difference ($p<0.001$) between the groups. Merely 5 patients in (A) and 3 patients in (B) were misdiagnosed. Figure 5.2 C presents the results of the assessment of the V/P SPECT images made by the clinical doctors. The results were similar to A and B, and there was a significant difference between the groups ($p<0.001$). The comparison between PAWP and the clinical report of the chest X-ray images regarding presence or absence of pulmonary congestion is shown in Figure 5.2 D. There was no difference between the groups ($p=0.79$) and there was an overlap. Several patients were misdiagnosed as not having pulmonary congestion on chest X-ray while they had an elevated PAWP.

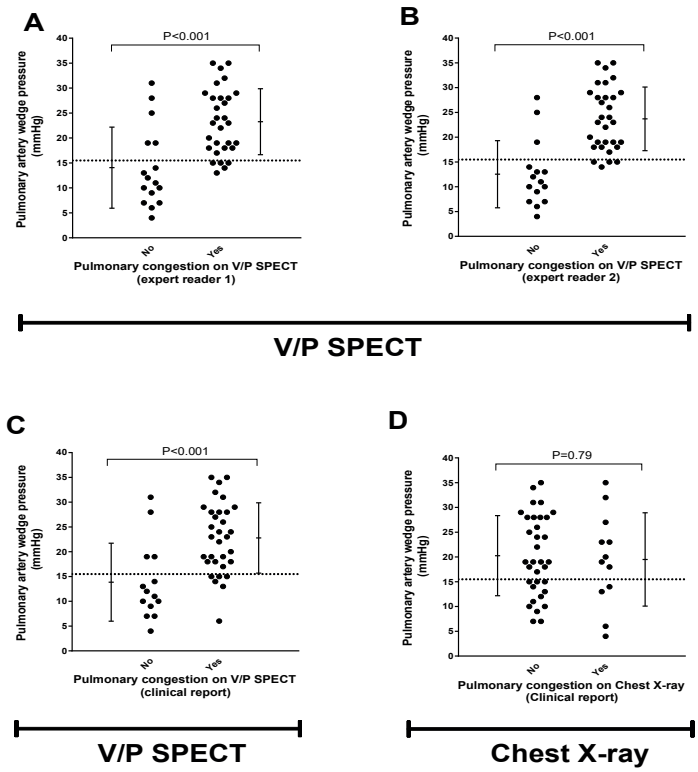

Figure 5.2: **A** and **B** show the assessment of expert reader 1 and 2 of the ventilation/perfusion single-photon emission computed tomography (V/P SPECT) images with regard to absence (no) or presence (yes) of pulmonary congestion, in comparison to pulmonary artery wedge pressure. The assessment made by the physicians in the clinical routine of the V/P SPECT images is shown in **C** and of the chest X-ray images shown in **D**, also with regard to presence and absence of pulmonary congestion.
The dashed lines represent the cut-off value of pulmonary artery wedge pressure > 15 mmHg for pulmonary congestion. The error bars represent mean ± 1 standard deviation.

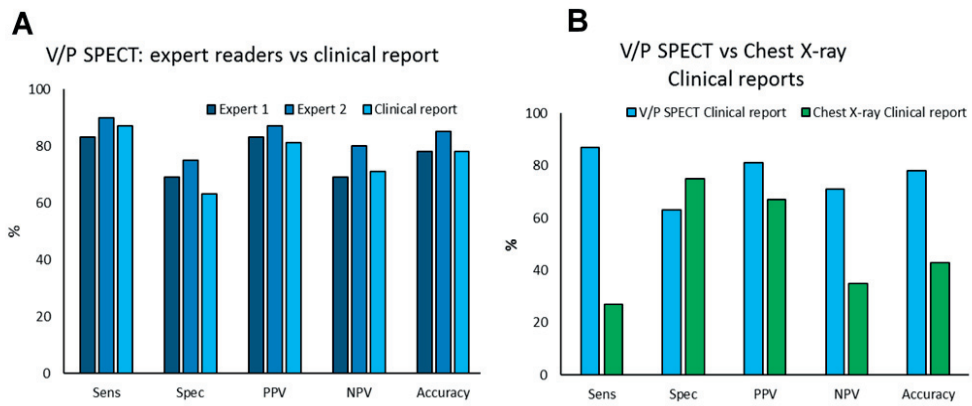

Figure 5.3: A. The diagnostic performance of the visual assessment of the ventilation/perfusion single-photon emission computed tomography (V/P SPECT) images made by expert reader 1, expert reader 2 and the clinical physicians, for the diagnosis of pulmonary congestion.
B. Shows the diagnostic performance of the visual assessment made by the clinical physicians of the V/P SPECT images (shown in blue) and by clinical radiology specialists of the chest X-ray images (shown in green).
The cut-off value of pulmonary artery wedge pressure that was used for the calculation was >15mmHg, for the diagnosis of pulmonary congestion.
Sens=sensitivity, spec=specificity, PPV=positive predictive value, NPV=negative predictive value.

Diagnostic accuracy

The results are presented in Figure 5.3 and the cut-off value for PAWP of >15 mmHg was used in the calculation of the sensitivity, specificity, PPV, NPV and accuracy. The diagnostic accuracy of the assessment of expert reader 1 of the V/P SPECT images with respect to presence or absence of pulmonary congestion was: sensitivity 83%, specificity 67%, PPV 83%, NPV 67% and accuracy 77%. For expert reader 2 the diagnostic accuracy of the assessment of the V/P SPECT images with respect to presence or absence of pulmonary congestion was as follows: sensitivity 90%, specificity 75%, PPV 87%, NPV 80% and accuracy 85%. The sensitivity, specificity, PPV, NPV and accuracy for the diagnostic accuracy of the clinical performance of V/P SPECT were: 87%, 63%, 81%, 71%, 78%, respectively. The clinical assessment of the chest X-ray images for the diagnosis of pulmonary congestion showed the following diagnostic accuracy: sensitivity 27%, specificity 75%, PPV 67%, NPV 35% and accuracy 43%, respectively.

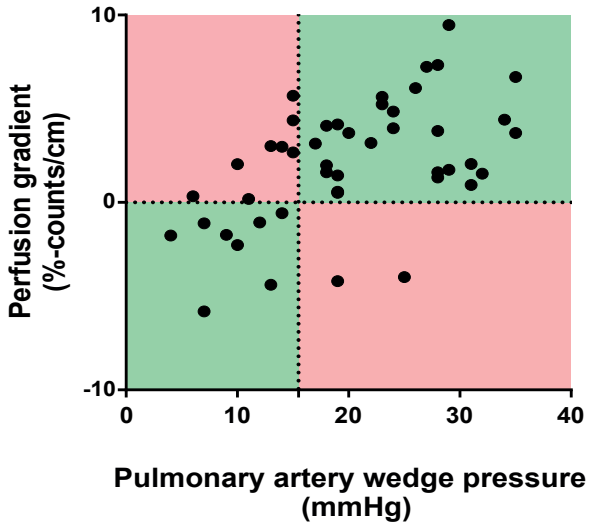

Figure 5.4: The perfusion gradients from ventilation/perfusion single-photon emission computed tomography (V/P SPECT) vs pulmonary artery wedge pressure from invasive right-heart catheterization. The red sections show patients with false diagnosis, and green sections patients with correct diagnosis. The dashed lines represent the cut-off values for pulmonary congestion: perfusion gradients 0%-counts/cm, and pulmonary artery wedge pressure >15 mmHg.

Agreement

There was a very good agreement between expert reader 1 and 2 in visually assessing the V/P SPECT images (k=0.85). When expert reader 2 reassessed the V/P SPECT images, the intra-individual agreement was perfect (k=1.0). There was a very good agreement between the assessment of expert reader 1 and the clinical report of V/P SPECT examination in assessing the V/P SPECT images (k=0.90). Furthermore, the agreement between expert reader 2 and the clinical report of V/P SPECT was good (k=0.75). The agreement between expert reader 2 who assessed the V/P SPECT images and the chest X-ray clinical report, with regard to presence/absence of pulmonary congestion was poor (k=0.12).

PAWP vs perfusion gradients

Figure 5.4 shows the PAWP and perfusion gradients. The red sections represent false diagnosis, and green sections represent correct diagnosis.
The patients who had negative (normal) perfusion gradients all had normal PAWP.
There were only two patients who had elevated PAWP (above 15 mmHg) who did not have positive (abnormal perfusion gradients). The rest of the patients who had elevated PAWP had positive perfusion gradients and were therefore correctly diagnosed as having pulmonary congestion.
The diagnostic accuracy of the perfusion gradients in the diagnosis of pulmonary conges-

tion is: sensitivity 93%, specificity 50%, PPV 78%, NPV 80% and accuracy 78%.

Summary

The main results from paper I show that perfusion gradients from V/P SPECT can be used to assess and quantify pulmonary congestion in heart failure. Furthermore, V/P SPECT had higher sensitivity and specificity than the recommended chest X-ray in the diagnosis of pulmonary congestion in heart failure.

5.2 Paper II: Perfusion gradients and PAWP before and after heart transplantation

In paper II, the perfusion gradients were investigated in patients before and after heart transplantation, and was validated against PAWP from right-heart catheterization.
Figure 5.5 presents perfusion SPECT images before and after heart transplantation. The redistribution of pulmonary perfusion seen before the transplantation is normalized after, likewise the perfusion gradients.

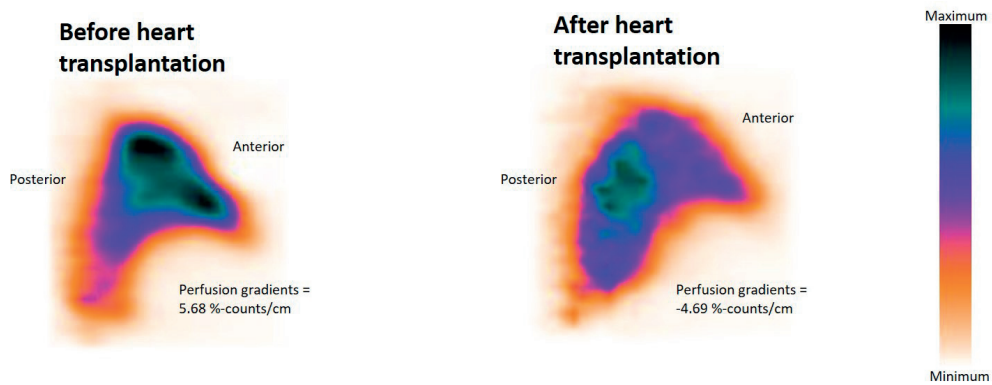

Figure 5.5: Perfusion images from ventilation/perfusion single-photon emission computed tomography (V/P SPECT), shown as sagital slices of the left lung, before and after heart transplantation. Note the normalized perfusion pattern and perfusion gradients after heart transplantation.

The difference in perfusion gradients in patients before (1.08 $\pm$ 2.87 %-counts/cm) and after (-2.11 $\pm$ 2.35 %-counts/cm) heart transplantation are presented in Figure 5.6 A. There was a statistically significant difference between patients before and after transplantation ($p<0.001$). Furthermore, the results were similar for PAWP before (20 $\pm$ 8 mmHg) and after (9 $\pm$ 5 mmHg) heart transplantation ($p<0.001$, Figure 5.6 B). The one patient that did not improve in perfusion gradients was the same that did not improve in PAWP.

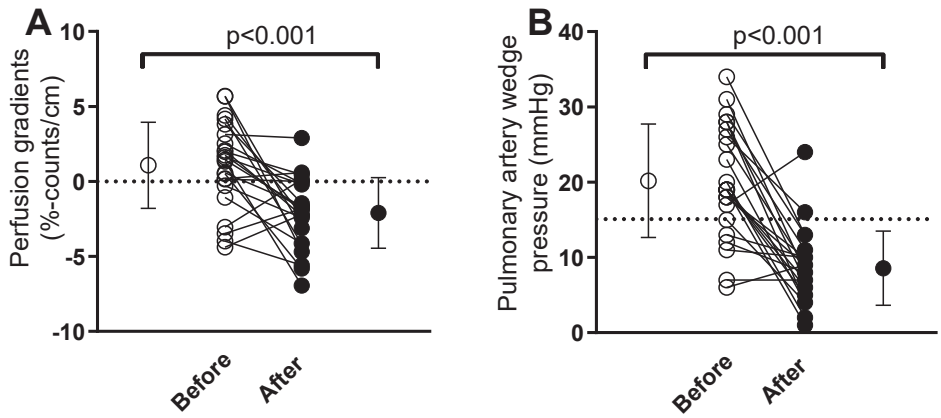

Figure 5.6: Perfusion gradients from ventilation/perfusion single-photon emission computed tomography (V/P SPECT) (A) and pulmonary artery wedge pressure (PAWP) from invasive right-heart catheterization (B) in patients before and after heart transplantation. Dashed lines represent the cut-off values for the diagnosis of pulmonary congestion (perfusion gradients (A)= 0%-counts/cm, PAWP (B)= >15 mmHg). Error bars represent mean ± standard deviation.

There was a correlation between perfusion gradients from V/P SPECT and PAWP from invasive right-heart catheterization, before (p=0.02, r=0.48, Figure 5.7 A) and after (p<0.001, r=0.68, Figure 5.7 B).

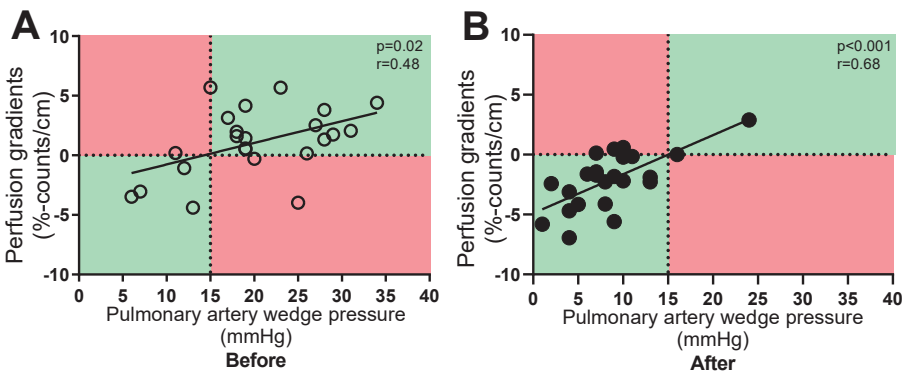

Figure 5.7: The perfusion gradients from ventilation/perfusion single-photon emission computed tomography (V/P SPECT) vs pulmonary artery wedge pressure (PAWP) from invasive right-heart catheterization before (A) and after (B) heart transplantation. The red sections show patients with false diagnosis, and green sections patients with correct diagnosis. The dashed lines represent the cut-off values for pulmonary congestion: perfusion gradients 0%-counts/cm, and PAWP >15 mmHg.

Summary

In summary, V/P SPECT is a non-invasive method that can be used in the follow-up of patients after heart transplantation.

5.3 Paper III: Perfusion gradients before and after CRT

Perfusion gradients from V/P SPECT. Figure 5.8 shows V/P SPECT images of a patient before and after CRT.

The perfusion gradients in patients with heart failure before CRT were -0.23 [-3.84-1.5]%-counts/cm, and were decreased after: -1.34 [-5.11-0.46] %-counts/cm, p=0.03, see Figure 5.9. As shown in Figure 5.10, thirteen out of nineteen patients (68%) showed improved perfusion gradients after CRT. Eleven out of the thirteen patients (85%) that presented an improvement in perfusion gradients also showed an improvement in functional capacity (NYHA-classification), p=0.0456, Figure 5.10. As shown in Figure 5.10, changes in the perfusion gradients were not associated with improvement in LVESV, LVEF and MLWHF, p=1.0, respectively.

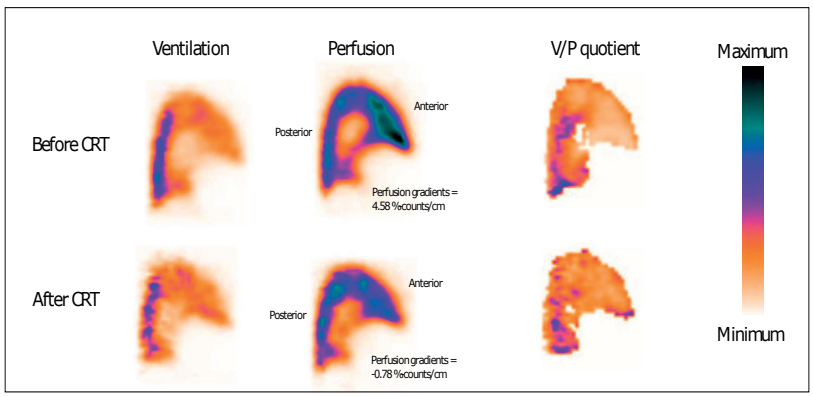

Figure 5.8: Ventilation/perfusion single-photon emission computed tomography (V/P SPECT) image of a patient before and after receiving cardiac resynchronization theraphy (CRT), with the corresponding perfusion gradients.

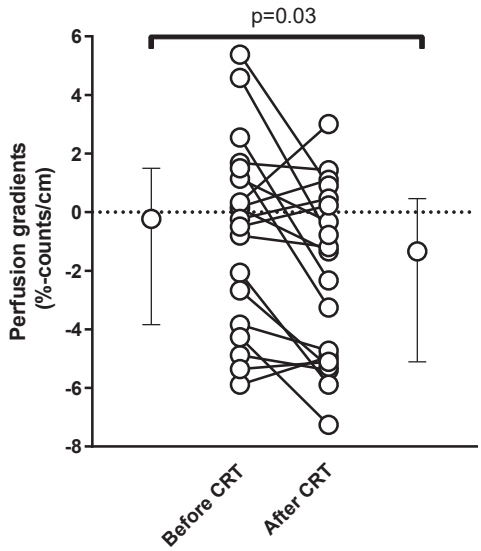

Figure 5.9: Perfusion gradients from ventilation/perfusion single-photon emission computed tomography (V/P SPECT) in patients with heart failure before and after cardiac resynchronization therapy (CRT). The dashed line represents the cut-off value for perfusion gradients (0%-counts/cm). Error bars represent median and inter quartile range.

	Perfusion gradients (improved)	Perfusion gradients (not improved)	P-value	LVESV (improved)	LVESV (not improved)	P-value
Improvement in NYHA (proportion of patients, N, %)	11/13=85%	2/6=33%	0.0456	6/7=86%	7/12=58%	0.3
Improvement in MLWHF (proportion of patients, N, %)	7/11=64% 2 patients missing	4/6=67%	1.0	5/7=71%	6/10=60% 2 patients missing	1.0
Improvement in LVEF (proportion of patients, N)	4/13=31%	1/6=17%	1.0	3/7=43%	2/12=17%	0.3
Improvement in LVESV (proportion of patients, N, %)	5/13=38%	2/6=33%	1.0	-	-	-
Improvement in perfusion gradients (proportion of patients, N, %)	-	-	-	5/7=71%	8/12=67%	1.0

Figure 5.10: Results of patients with improved and non-improved perfusion gradients vs New York Heart Association (NYHA)-classification, quality of life scoring system Minnesota living with heart failure (MLWHF), left ventricular ejection fraction (LVEF) and left ventricular end-systolic volume (LVESV), as well as improved and non-improved LVESV vs NYHA-classification, MLWHF, LVEF and perfusion gradients.

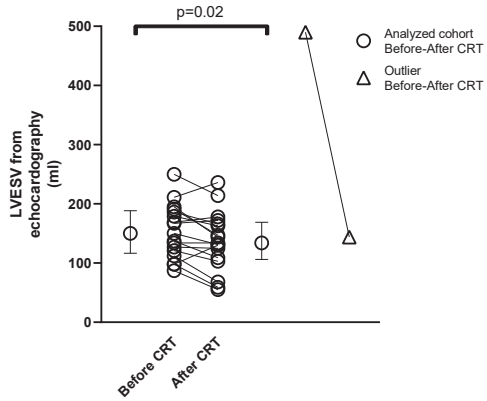

Figure 5.11: Left ventricular end-systolic volume (LVESV) from echocardiography in patients with heart failure before and after cardiac resynchronization therapy (CRT). Error bars represent median and inter quartile range. The white triangle represents an outlier.

LVESV from echocardiography. The LVESV was 159 [119-192] ml in patients with heart failure before receiving CRT, and was decreased after CRT, 139 [108-168] ml, n=18, p=0.02, see Figure 5.11. Thirty-seven percent (7/19) of the patients presented with improved LVESV after the treatment. Changes in LVESV were not associated with improvement in perfusion gradients (p=1.0), LVEF (p=0.3), MLWHF (p=1.0) and NYHA-classification (p=0.3), as presented in Figure 5.10.

Summary

In summary, the perfusion gradients from V/P SPECT were improved in the majority of the patients after receiving CRT. Only 37% of the patients showed improvement in LVESV, while 68% showed improvement in perfusion gradients. Improvement in perfusion gradients was associated with improvement in NYHA-classification, while improvement in LVESV from echocardiography was not associated with improvement with any other variable.

5.4 Paper IV: PBVV

In paper IV, PBVV and $PBVV_{SV}$ were significantly higher in patients with heart failure compared to healthy controls (45 $\pm$ 15 ml vs. 34 $\pm$ 9 ml, p=0.02 and 58 $\pm$ 14 % vs. 43 $\pm$ 7 %, p<0.001), as presented in Figure 5.12.

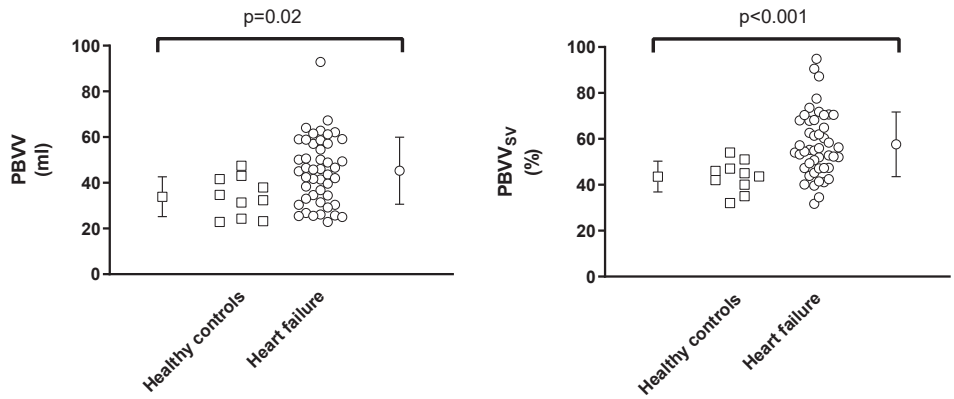

Figure 5.12: The pulmonary blood volume variation, PBVV (to the left) and PBVV indexed to stroke volume, $PBVV_{SV}$ (to the right) in healthy controls (squares) and patients with heart failure (circles). Error bars represent mean $\pm$ standard deviation.

LV contribution to SV

Patients with heart failure had lower LVAVPD, compared to healthy controls (8.5 $\pm$ 3.7 mm vs. 14.2 $\pm$ 1.9 mm, p<0.001).

The change in the product of the LV area times LVAVPD could be dependent on the volume from the pulmonary veins that enter the left atrium. As shown in Figure 5.13 A and B, the results were (R^2= 0.80, p<0.001, n = 10) in healthy controls, and (R^2= 0.59, p<0.001, n = 45) in patients with heart failure.

The definition of the LV longitudinal contribution to SV is the LV area times LVAVPD as a percentage of the SV in the main pulmonary. The LV longitudinal contribution to SV could be determined by the change in $PBVV_{SV}$ in patients with heart failure (R^2= 0.15, p = 0.02, n = 36, Figure 5.13 D. However, the LV longitudinal contribution to SV cannot be determined by the change in $PBVV_{SV}$ in healthy controls (R^2<0.01, p = 0.92, n =8, Figure 5.13 C).

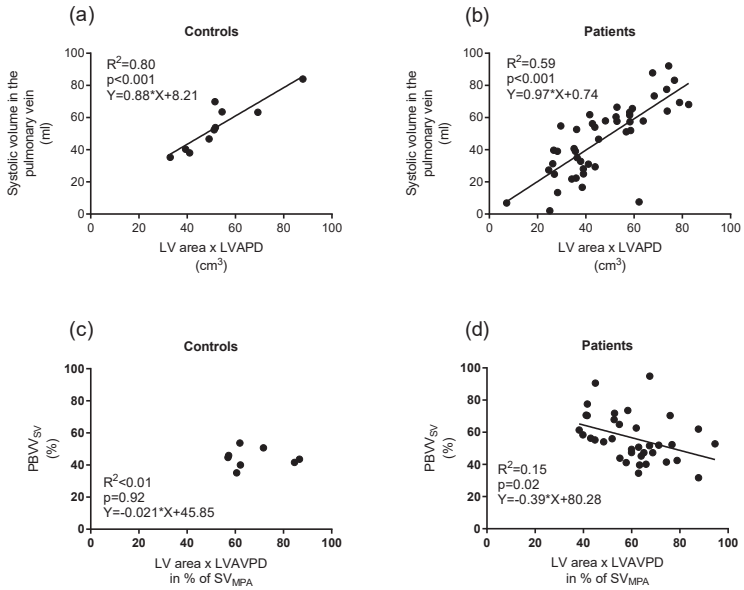

Figure 5.13: Correlation between the systolic volume in the pulmonary vein and the left ventricular (LV) area times (x) LV atrioventricular-plane displacement (LVAPD) in 10 healthy controls (**a**) and 45 patients with heart failure (**b**). Correlation between pulmonary blood volume variation indexed to effective stroke volume ($PBVV_{SV}$) and LV area x LVAVPD as a percentage of the stroke volume (SV) in the main pulmonary artery (MPA) (LV longitudinal contribution to SV) in 8 healthy controls (**c**) and 36 patients with heart failure (**d**). The measurements and calculations were performed using magnetic resonance imaging. The black lines represent the fitted linear regression line.

Phase shift

In healthy controls, the phase shift between pulmonary in- and outflow could not explain the change in $PBVV_{SV}$ (R^2 = 0.04, p=0.65, n = 8, Figure 5.14 a). In patients with heart failure, on the other hand, the change in $PBVV_{SV}$ could be explained by the phase shift (R^2= 0.31, p<0.001, n = 36, Figure 5.14 b). A difference was found in phase shift between patients with $PBVV_{SV} \leq 57\%$ and those with $PBVV_{SV} > 57\%$ (29 ± 6 vs. $40 \pm 9\%$, p<0.001, n = 36, Figure 5.14 c).

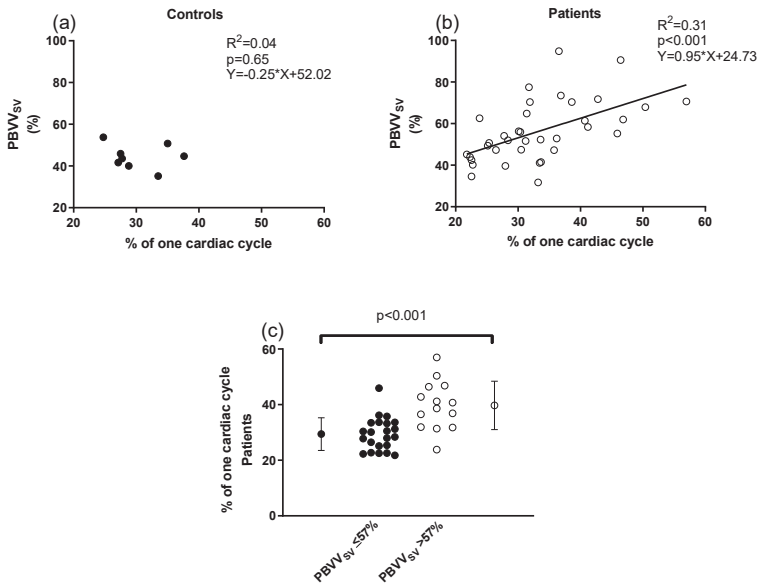

Figure 5.14: Correlation between pulmonary blood volume variation indexed to stroke volume ($PBVV_{SV}$) and phase shift between in- and outflow (the time point for when the maximum PBVV occurs as a percentage of the cardiac cycle) in healthy controls (**a**) and patients with heart failure (**b**). The black line in b represents the fitted regression line. Panel (**c**) represents the phase shift between pulmonary in- and outflow in patients with $PBVV_{SV} \leq 57\%$ and patient >57%. Error bars represent mean $\pm$ standard deviation.

Vessel area variation

In patients with heart failure and healthy controls, the area variation of the main pulmonary artery could not explain the change in $PBVV_{SV}$ (R^2= 0.10, p= 0.07, n = 36, and R^2= 0.05, p= 0.60, n = 8). The same applies to the pulmonary vein (patients with heart failure: R^2= 0.01, p= 0.74, healthy controls: R^2= 0.38, p= 0.10).

Flow measurements. The intra-observer variability was performed by one observer for the delineations of the main pulmonary artery, the pulmonary vein, as well as for the calculation of PBVV and $PBVV_{SV}$. The inter-observer variability was performed by two observers for the same delineations as for the intra-observer analysis. Table 5.1 presents the results. The only bias that was found was in the delineations of the pulmonary vein, where the blood flow in the vein was underestimated (due to a missing part of the vessel). Our results show that this will not affect the calculation of PBVV and $PBVV_{SV}$, since the correct flow profile is more important than the total flow in the vessel. When the flow is lower in a vessel, a larger factor will be obtained that the venous flow profile is multiplied with (arterial

flow/venous flow).
There was a small bias in the delineation of the pulmonary artery, as well as in the calculation of PBVV and $PBVV_{SV}$, which can be interpreted as that the $PBVV_{SV}$ is an observer-independent measure.

Table 5.1: Results from intra- and interobserver variability analysis on 10 patients with heart failure for the delineations of the main pulmonary artery and pulmonary vein, as well as the calculation of pulmonary blood volume variation (PBVV) and PBVV indexed to stroke volume (SV) ($PBVV_{SV}$).

	Intra-observer variability		**Inter-observer variability**	
	Bias	R^2	**Bias**	R^2
Main pulmonary artery (ml)	-3.88 $\pm$ 4.73	0.95	-0.24 $\pm$ 4.61	0.96
Pulmonary vein (ml)	-2.03 $\pm$ 4.07	0.81	2.42 $\pm$ 6.39	0.57
PBVV (ml)	-1.89 $\pm$ 2.53	0.99	-0.35 $\pm$ 2.60	0.99
$PBVV_{SV}$ (%)	0.48 $\pm$ 2.55	0.96	0.04 $\pm$ 2.64	0.96

Mechanisms behind increased $PBVV_{SV}$

A multiple regression analysis was performed in order to investigate what variables could explain the variation behind $PBVV_{SV}$ in patients with heart failure. The results are presented in Table 5.2. The LV longitudinal contribution to SV and phase shift between in- and outflow were the variables that were included in the multiple regression analysis. These two variables predicted and explained the variation behind $PBVV_{SV}$ with an R^2 value of 0.38, meaning that approximately 40% of the variation in the PBVV could be explained by the two variables. However, according to the table, the p-value of the the LV longitudinal contribution to SV was 0.06, which means that this variable did not contribute to the multiple regression analysis model. Therefore, the phase shift alone predicted the model with an R^2 value of 0.31 (p<0.001), which is approximately 30%.

Table 5.2: Results from multiple regression analysis

Multiple regression analysis results			
Predictors	R^2**-value (for all predictors)**	β **-value**	**P-value**
$PBVV_{SV}$			
LV longitudinal contribution to SV	0.38	-0.27	0.06
Phase shift between in- and outflow		0.50	0.001

Summary

In summary, $PBVV_{SV}$ was increased in patients with heart failure, compared to healthy controls. The mechanism behind the change in $PBVV_{SV}$ in patients could be explained by the LV contribution to SV and the phase shift between pulmonary in- and outflow. The change in PBVV could not be explained by the vessel area variation. There was no difference in the calculation of $PBVV_{SV}$, when using breath hold or free-breathing sequences. Furthermore, there was no difference when using only one pulmonary vein versus all pulmonary veins in the calculation of $PBVV_{SV}$.

Chapter 6

Discussion

The results of this thesis have increased the knowledge and understanding behind the physiology and pathophysiology of heart failure.

This thesis has shown that V/P SPECT, validated against PAWP from invasive right-heart catheterization, can be used in the diagnosis of pulmonary congestion in heart failure, and can therefore be a surrogate measure of PAWP. According to guidelines [1] [39], the recommended non-invasive method in diagnosing pulmonary congestion in heart failure is chest X-ray. However, despite the knowledge of its low sensitivity in the diagnosis [39] [42] [43], it is still used, and no other method has been able to replace it in heart failure diagnosis. However, in this thesis V/P SPECT was compared to chest X-ray and was shown to be superior to chest X-ray in the diagnosis of pulmonary congestion in heart failure. Pulmonary edema in heart failure affects the pulmonary perfusion pattern (West zones) [8] and can be visualized and quantified using V/P SPECT. The advantage with V/P SPECT is that it shows a physiological map of the lungs meanwhile chest X-ray shows the anatomy.

The exact reason behind the redistribution of pulmonary perfusion from posterior to anterior or lower to upper parts of the lungs, depending on body position, is unknown. However, a suggested hypothesis propose that it occurs in the interstitial parts of the lung [24] [25] [26] [27] [28]. During normal conditions, blood flow is distributed mainly to the lower parts of the lungs where the alveoli are also more open [8]. In the condition of heart failure with pulmonary congestion, an outflow of fluid is seen into the interstitium. The accumulation of fluid in the interstitium is influenced by gravity and the small vessels and capillaries within the interstitium in lower located parts of the lungs become less distensible and compressed. This will in turn affect the interaction between the capillaries and alveoli, which results in a thicker membrane of the alveoli and therefore a decreased gas exchange [82]. As the vessels close in the lower parts of the lungs, redirection of pulmonary perfusion to less dependent parts of the lungs is seen.

In this thesis, patients with heart failure showed redistribution of pulmonary perfusion from posterior to anterior parts of the lungs, where the results were confirmed by elevated LAP (PAWP). The observation of the change in distribution of pulmonary blood flow in certain conditions started more than 50 years ago. Patients with mitral valve disease (which is one of the causes of LV failure) were studied with regards to the distribution of pulmonary blood flow (perfusion) [83] [84] using radioactive isotopes. It was shown that these patients have a redistribution of the blood flow from the lower to upper parts of the lungs, which was the opposite condition of the distribution of the blood flow in a normal person. The results in these patients were correlated to elevated pulmonary venous pressure and mean LAP. The redistribution of pulmonary blood flow was also found among patients with chronic obstructive pulmonary disease in combination with heart disease [85] and patients with chronic congestive heart failure/ischemic heart disease [86] [87]. In another study, 69 patients with congestive heart failure were examined with lung scintigraphy and chest X-ray [88]. Different patterns were found with lung scintigraphy, the most common were irregular pattern and redistribution of the pulmonary perfusion to upper parts. Other patterns were focal, non-segmental perfusion defects. The perfusion pattern seen in lung scintigraphy was not consistent with chest X-ray in these patients.
Lung scintigraphy, was the first method used to assess the distribution of pulmonary ventilation and perfusion in a 2D manner. Lately, the field of nuclear medicine imaging has evolved and improved resulting in the possibility to attain a 3D assessment of the pulmonary ventilation and perfusion via tomographic lung scintigraphy, V/P SPECT. In 2008, co-workers from the Department of Clinical Physiology in Lund, Sweden showed that V/P SPECT can be used to investigate and quantify the distribution of pulmonary perfusion in patients with heart failure [61]. The study was performed retrospectively in patients admitted due to suspicion of pulmonary embolism. Fifteen percent of these patients had heart failure and signs of pulmonary congestion (redistribution of pulmonary perfusion from posterior to anterior parts of the lungs). These patients also showed positive perfusion gradients. In this study there were also examples of normalized perfusion pattern and perfusion gradients after anticongestive treatment. Thus, this needed to be validated. A continuation and validation of the study from 2008 is the work performed in this thesis, where it was shown that quantification and diagnosis of heart failure can be performed using V/P SPECT. This was also validated with the reference method invasive right-heart catheterization. West et al [8] have previously shown that the lungs functionally consist of different zones, where there is more blood flow in the lower located part of the lungs [8]. In this thesis, we have obtained similar result as West et al and visualized it with tomographic lung scintigraphy and validated the method with PAWP measurements.

In this thesis, it was shown that V/P SPECT can be used to follow-up treatment effect after heart transplantation, as validated by PAWP from invasive right-heart catheterization. Furthermore, V/P SPECT was also improved after CRT. In addition, the majority of patients showed improvement in perfusion gradients from V/P SPECT after receiving CRT,

compared to LVESV. Improved perfusion gradients from V/P SPECT were also more associated to the patient's functional capacity (NYHA-classification). To follow-up any treatment effect non-invasively is necessary and needed option.
Furthermore, in this thesis, the PBVV was higher in patients with heart failure compared to healthy controls. Prior to this thesis, PBVV had never been investigated in patients with heart failure. It was previously studied in pigs following acute myocardial infarction, where the PBVV was found to be decreased [76]. The original theory behind the decrease was that the vessels in the lungs are stiff and not distensible since they were already stretched. Other explanations may be due to the activation of the sympathetic nervous system and increased endothelin (which is a vasoconstrictor) secretion that results in constriction of the pulmonary arteries. Also, the pigs were healthy and young before the infarction and their compensatory mechanisms were normal. The LAP was not affected in the previous work with the pigs [76]. The mechanisms behind the increased PBVV in patients with heart failure is unknown. However, different hypotheses were made and studied in this thesis and resulted in the following and shown in Figure 6.1:

- It is known that the LAP is usually affected and elevated in patients with heart failure [89] and leads to a decreased pulmonary venous flow during systole [90].
- The theory is that the vessels in the lungs are more distensible due to the windkessel effect. These vessels can be bigger and therefore result in a variation of the blood flow.
- PBVV could be a measure of the LV function. In this study (paper IV), there was a relationship between the systolic volume in the pulmonary vein (which is the volume of blood that enters the left atrium via the pulmonary veins during systole) and the LV systolic longitudinal shortening. This was also seen in a previous study [78]. It is known that the movement of the AV-plane affects the flow profile in the pulmonary vein [91]. What really happens is that a downward (descending) movement of the LV AV-plane during systole result in that the pressure in the left atrium is decreased. This creates a pressure gradient (suction) of the blood flow from the pulmonary veins to the left atrium [78].
- The phase shift between pulmonary in- and outflow could be due to that during normal conditions, the RV pumps blood during systole, and at the same time the LV "sucks" the blood from the pulmonary veins. In the condition of heart failure, the suction of the blood by the LV occurs later and more slowly. Additionally, morphology of the flow profiles of the pulmonary artery and vein affects this measure.
- We also investigated if there was a correlation between PBVV and large vessel area variation (main pulmonary artery and pulmonary vein). As there was no difference in either patients with heart failure nor healthy controls, we speculate that the rest of the variation occurs on a small vessel level (where we cannot measure); in the capillaries,

venules and arterioles. However, it has previously been seen that approximately 60% of the SV is owing to small capillaries and arteries [92], which is compatible to the results in this study.

PBVV is a novel way to study the lungs and the pulmonary circulation using MRI. It is a promising method in the assessment of patients with heart failure. It reflects the maximum variation of blood flow in the pulmonary circulation. MRI is a non-invasive method that has and is still being developed to be used in investigating blood flow.

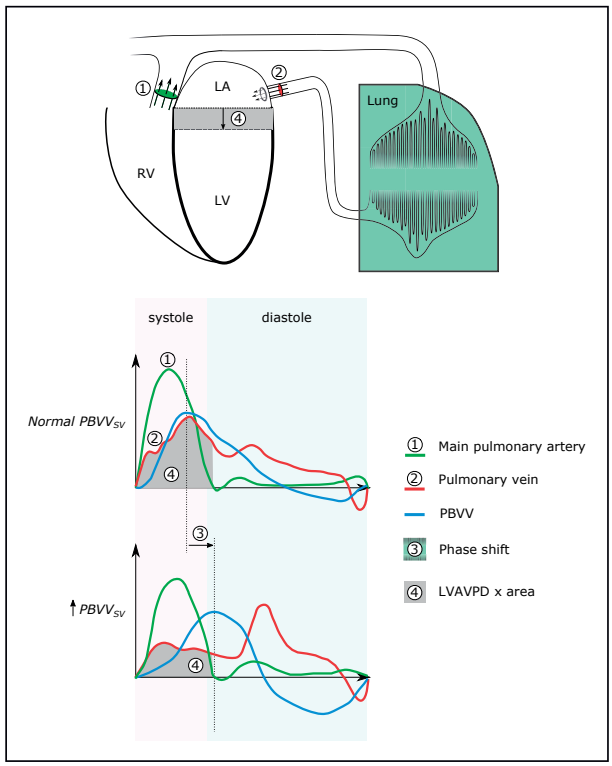

Figure 6.1: A schematic image of the mechanisms behind the pulmonary blood volume variation indexed to the stroke volume (PBVV$_{SV}$) in patients with heart failure. The green curve represents the flow in the main pulmonary artery, the red curve represents the flow in the pulmonary vein and the blue curve represents the PBVV, during normal (upper graph) and increased (lower) PBVV$_{SV}$. Number 3 represents the phase shift between pulmonary in- and out flow and number 4 represents the left ventricular (LV) longitudinal contribution to SV.

6.1 Future direction

Future studies are to validate PBVV with PAWP from invasive right-heart catheterization, and to investigate it in different patient populations such as pulmonary hypertension and patients with congenital heart disease. This will increase our understanding in the physiology behind the diseases. In addition, it will also be interesting to investigate the PBVV before and after a treatment. Furthermore, it would be of interest to study the perfusion gradients in all ages and both genders (retrospectively) in order to observe the spread and distribution of the values.

Chapter 7

Conclusions

The specific conclusions of each paper was:

Paper I: V/P SPECT can be used as a non-invasive method to diagnose and quantify pulmonary congestion in patients with heart failure and is more accurate than chest X-ray in diagnosing pulmonary congestion in the clinical setting.

Paper II: V/P SPECT is a promising method for objective assessment and quantification of treatment effects in patients with heart failure after heart transplantation. Although V/P SPECT cannot replace right-heart catheterization, it could be a noninvasive and useful method in selected cases to guide treatment and catheterization during follow-up. V/P SPECT could also be a user-independent tool to quantitatively evaluate results of anticongestive treatment in clinical trials.

Paper III: Perfusion gradients from V/P SPECT is a promising quantitative, user-independent method in the assessment of CRT response in patients with heart failure. The study demonstrated an improvement of perfusion gradients in a larger proportion of the patients after CRT compared to echocardiography. Moreover, improved perfusion gradients were associated with an improvement of patients' functional capacity, according to NYHA. Perfusion gradients could have an added value to the currently used diagnostic methods in the follow-up of patients with heart failure after receiving CRT.

Paper IV: The $PBVV_{SV}$ is higher in patients with heart failure compared with healthy controls. Approximately 40% of the variation of $PBVV_{SV}$ in patients with heart failure can be explained by the LV longitudinal contribution to SV and the phase shift between the pulmonary in- and outflow, where the phase shift alone accounts for approximately 30% of the variation. Because the large vessel distensibility does not differ, the remaining variation (60–70%) is suggested to occur on the small vessel level. Future studies are needed to show the clinical added value of $PBVV_{SV}$ in comparison to invasive measurements of the LAP.

Chapter 8

References

[1] Ponikowski P., Voors A. A., Anker S. D., Bueno H., Cleland J. G., Coats A. J., Falk V., González-Juanatey J. R., Harjola V. P., Jankowska E. A., Jessup M., Linde C., Nihoyannopoulos P., Parissis J. T., Pieske B., Riley J. P., Rosano G. M., Ruilope L. M., Ruschitzka F., Rutten F. H., van der Meer P., Filippatos G., McMurray J. J., Aboyans V., Achenbach S., Agewall S., Al-Attar N., Atherton J. J., Bauersachs J., Camm A. J., Carerj S., Ceconi C., Coca A., Elliott P., Erol Ö., Ezekowitz J., Fernández-Golfín C., Fitzsimons D., Guazzi M., Guenoun M., Hasenfuss G., Hindricks G., Hoes A. W., Iung B., Jaarsma T., Kirchhof P., Knuuti J., Kolh P., Konstantinides S., Lainscak M., Lancellotti P., Lip G. Y., Maisano F., Mueller C., Petrie M. C., Piepoli M. F., Priori S. G., Torbicki A., Tsutsui H., van Veldhuisen D. J., Windecker S., Yancy C., and Zamorano J. L. 2016 ESC Guidelines for the diagnosis and treatment of acute and chronic heart failure. *European Journal of Heart Failure*, 18(8):891–975, 2016.

[2] Chase S. C., Wheatley C. M., Olson L. J., Beck K. C., Wentz R. J., Snyder E. M., Taylor B. J., and Johnson B. D. Impact of chronic systolic heart failure on lung structure–function relationships in large airways. *Physiological Reports*, 4(13):1–11, 2016.

[3] Weiss K., Schär M., Panjrath G. S., Zhang Y., Sharma K., Bottomley P. A., Golozar A., Steinberg A., Gerstenblith G., Russell S. D., and Weiss R. G. Fatigability, Exercise Intolerance, and Abnormal Skeletal Muscle Energetics in Heart Failure. *Circulation: Heart Failure*, 10(7):1–12, 2017.

[4] Hall J. E. *Guyton and hall textbook of medical physiology thirteenth edition*. Elsevier, 2011.

[5] Widmaier E. P., Raff H., and Strang K. T. *Vander's Human Physiology: the mechanism of body function*. McGraw-Hill Education, 2004.

[6] Miserocchi G., Negrini D., Del Fabbro M., and Venturoli D. Pulmonary interstitial pressure in intact in situ lung: Transition to interstitial edema. *Journal of Applied Physiology*, 74(3):1171–1177, 1993.

[7] Negrini D., Passi A., De Luca G., and Miserocchi G. Pulmonary interstitial pressure and proteoglycans during development of pulmonary edema. *American Journal of Physiology - Heart and Circulatory Physiology*, 270(6 39-6), 1996.

[8] West J. B., Dollery C. T., and Naimark A. Distribution of Blood Flow in Isolated Lung; Relation To Vascular and Alveolar Pressure. *Journal of applied physiology*, 19: 713–724, 1964.

[9] Hughes J. M., Glazier J. B., Maloney J. E., and West J. B. Effect of lung volume on the distribution of pulmonary blood flow in man. *Respiration Physiology*, 4(1):58–72, 1968.

[10] Kanski M. *Non-invasive measures of heart failure*. PhD thesis, Lund University, Sweden, 2015.

[11] Mosterd A. and Hoes A. W. Clinical epidemiology of heart failure. *Heart*, 93(9): 1137–1146, 2007.

[12] Roger V. L. Epidemiology of heart failure. *Circulation Research*, 113(6):646–659, 2013.

[13] Kannel W. B. and Belanger A. J. Epidemiology of heart failure. *American Heart Journal*, 121(3 PART 1):951–957, 1991.

[14] Wilkins E., Wilson L., Wickramasinghe K., and Bhatnagar P. European Cardiovascular Disease Statistics 2017. *European Heart Network*, 2017.

[15] WHO. Cardiovascular diseases https://www.who.int/health-topics/cardiovascular-diseases/#tab=tab_1, 2020.

[16] Braunwald E. *Heart disease: A textbook of Cardiovascular Medicine*. W.B Saunders company, 4th edition, 1992.

[17] Mebazaa A., Yilmaz M. B., Levy P., Ponikowski P., Peacock W. F., Laribi S., Ristic A. D., Lambrinou E., Masip J., Riley J. P., McDonagh T., Mueller C., Defilippi C., Harjola V. P., Thiele H., Piepoli M. F., Metra M., Maggioni A., McMurray J., Dickstein K., Damman K., Seferovic P. M., Ruschitzka F., Leite-Moreira A. F., Bellou A., Anker S. D., and Filippatos G. Recommendations on pre-hospital & early hospital management of acute heart failure: A consensus paper from the Heart Failure Association of the European Society of Cardiology, the European Society of Emergency Medicine and the Society of Academic Emergenc. *European Journal of Heart Failure*, 17(6):544–548, 2015.

[18] Carabello B. A. Evolution of the study of left ventricular function: Everything old is new again. *Circulation*, 105(23):2701–2703, 2002.

[19] Curtis J. P., Sokol S. I., Wang Y., Rathore S. S., Ko D. T., Jadbabaie F., Portnay E. L., Marshalko S. J., Radford M. J., and Krumholz H. M. The association of left ventricular ejection fraction, mortality, and cause of death in stable outpatients with heart failure. *Journal of the American College of Cardiology*, 42(4):736–742, 2003.

[20] Sanderson J. Heart failure with a normal ejection fraction. *Heart*, 93(2):155–158, 2007.

[21] Patterson S. W., Piper H., and Starling E. H. The regulation of the heart beat. *The Journal of Physiology*, 48(6):465–513, 1914.

[22] Patterson S. W. and Starling E. H. On the mechanical factors which determine the output of the ventricles. *The Journal of Physiology*, 48(5):357–379, 1914.

[23] Frank O. On the dynamics of cardiac muscle. *American Heart Journal*, 58(2):282–317, 1959.

[24] Staub N. C., Nagano H., and Pearce M. L. Pulmonary edema in dogs, especially the sequence of fluid accumulation in lungs. *Journal of applied physiology*, 22(2):227–240, 1967.

[25] Staub N. C. The forces regulating fluid filtration in the lung. *Microvascular Research*, 15(1):45–55, 1978.

[26] Chinard F. P. Starling's hypothesis in the formation of edema. *Bulletin of the New York Academy of Medicine*, 38:375–389, 1962.

[27] Starling E. H. On the Absorption of Fluids from the Connective Tissue Spaces. *The Journal of Physiology*, 19(4):312–326, 1896.

[28] Fishman A. P. Pulmonary edema. The water-exchanging function of the lung. *Circulation*, 46(2):390–408, 1972.

[29] Guyton A. C. and Lindsey A. W. Effect of elevated left atrial pressure and decreased plasma protein concentration on the development of pulmonary edema. *Circulation research*, 7(4):649–657, 1959.

[30] Goldman L., Cook E. F., Mitchell N., Flatley M., Sherman H., and Cohn P. F. Pitfalls in the serial assessment of cardiac functional status. How a reduction in "ordinary" activity may reduce the apparent degree of cardiac compromise and give a misleading impression of improvement. *Journal of Chronic Diseases*, 35(10):763–771, 1982.

[31] Stewart G. C. and Givertz M. M. Mechanical circulatory support for advanced heart failure: Patients and technology in evolution. *Circulation*, 125(10):1304–1315, 2012.

[32] Cazeau S., Leclercq C., Lavergne T., Walker S., Varma C., Linde C., Garrigue S., Kappenberger L., Haywood G. A., Santini M., Bailleul C., Mabo P., Lazarus A., Ritter P., Levy T., McKenna W., and Daubert J.-C. Effects of Multisite Biventricular Pacing in Patients with Heart Failure and Intraventricular Conduction Delay. *New England Journal of Medicine*, 344(12):873–880, 2001.

[33] Cleland J. G., Daubert J. C., Erdmann E., Freemantle N., Gras D., Kappenberger L., and Tavazzi L. Longer-term effects of cardiac resynchronization therapy on mortality in heart failure [the CArdiac REsynchronization-Heart Failure (CARE-HF) trial extension phase]. *European Heart Journal*, 27(16):1928–1932, 2006.

[34] Cleland J. G., Freemantle N., Erdmann E., Gras D., Kappenberger L., Tavazzi L., and Daubert J. C. Long-term mortality with cardiac resynchronization therapy in the Cardiac Resynchronization-Heart Failure (CARE-HF) trial. *European Journal of Heart Failure*, 14(6):628–634, 2012.

[35] Sohaib S. M., Finegold J. A., Nijjer S. S., Hossain R., Linde C., Levy W. C., Sutton R., Kanagaratnam P., Francis D. P., and Whinnett Z. I. Opportunity to Increase Life Span in Narrow QRS Cardiac Resynchronization Therapy Recipients by Deactivating Ventricular Pacing: Evidence From Randomized Controlled Trials. *JACC: Heart Failure*, 3(4):327–336, 2015.

[36] Cleland J. G., Abraham W. T., Linde C., Gold M. R., Young J. B., Claude Daubert J., Sherfesee L., Wells G. A., and Tang A. S. An individual patient meta-analysis of five randomized trials assessing the effects of cardiac resynchronization therapy on morbidity and mortality in patients with symptomatic heart failure. *European Heart Journal*, 34(46):3547–3556, 2013.

[37] Bakos Z., Markstad H., Ostenfeld E., Carlsson M., Roijer A., and Borgquist R. Combined preoperative information using a bullseye plot from speckle tracking echocardiography, cardiac CT scan, and MRI scan: Targeted left ventricular lead implantation in patients receiving cardiac resynchronization therapy. *European Heart Journal Cardiovascular Imaging*, 15(5):523–531, 2014.

[38] Allison J. D., Flickinger F. W., Wright J. C., Falls D. G., Michael Prisant L., VonDohlen T. W., and Frank M. J. Measurement of left ventricular mass in hypertrophic cardiomyopathy using MRI: Comparison with echocardiography. *Magnetic Resonance Imaging*, 11(3):329–334, 1993.

[39] Yancy C. W., Jessup M., Bozkurt B., Butler J., Casey D. E., Drazner M. H., Fonarow G. C., Geraci S. A., Horwich T., Januzzi J. L., Johnson M. R., Kasper E. K., Levy W. C., Masoudi F. A., McBride P. E., McMurray J. J., Mitchell J. E., Peterson P. N., Riegel B., Sam F., Stevenson L. W., Tang W. H., Tsai E. J., and Wilkoff B. L. 2013 ACCF/AHA guideline for the management of heart failure: A report of the american college of cardiology foundation/american heart association task force on practice guidelines. *Circulation*, 128(16):147–239, 2013.

[40] Hawkins N. M., Petrie M. C., Jhund P. S., Chalmers G. W., Dunn F. G., and McMurray J. J. Heart failure and chronic obstructive pulmonary disease: Diagnostic pitfalls and epidemiology. *European Journal of Heart Failure*, 11(2):130–139, 2009.

[41] Thomas J. T., Kelly R. F., Thomas S. J., Stamos T. D., Albasha K., Parrillo J. E., and Calvin J. E. Utility of history, physical examination, electrocardiogram, and chest radiograph for differentiating normal from decreased systolic function in patients with heart failure. *American Journal of Medicine*, 112(6):437–445, 2002.

[42] Collins S. P., Lindsell C. J., Storrow A. B., and Abraham W. T. Prevalence of negative chest radiography results in the emergency department patient with decompensated heart failure. *Annals of Emergency Medicine*, 47(1):13–18, 2006.

[43] Chakko S., Woska D., Martinez H., Marchena E. D., Futterman L., Kessler K. M., and Myerburg R. J. Clinical, radiographic, and hemodynamic correlations in chronic congestive heart failure: Conflicting results may lead to inappropriate care. *The American Journal of Medicine*, 90(1):353–359, 1991.

[44] Kataoka H. and Takada S. The role of thoracic ultrasonography for evaluation of patients with decompensated chronic heart failure. *Journal of the American College of Cardiology*, 35(6):1638–1646, 2000.

[45] Costanzo W. E. and Fein S. A. The role of the chest X-ray in the evaluation of chronic severe heart failure: Things are not always as they appear. *Clinical Cardiology*, 11(7): 486–488, 1988.

[46] Galiè N., Humbert M., Vachiery J. L., Gibbs S., Lang I., Torbicki A., Simonneau G., Peacock A., Noordegraaf A. V., Beghetti M., Ghofrani A., Sanchez M. A. G., Hansmann G., Klepetko W., Lancellotti P., Matucci M., McDonagh T., Pierard L. A., Trindade P. T., Zompatori M., and Hoeper M. 2015 ESC/ERS Guidelines for the diagnosis and treatment of pulmonary hypertension. *European Respiratory Journal*, 46(4):903–975, 2015.

[47] Grymuza M., Malaczynska-Rajpold K., Jankiewicz S., Siniawski A., Grygier M., Mitkowski P., Kaluzna-Oleksy M., Lesiak M., Mularek-Kubzdela T., and Araszkiewicz A. Right heart catheterization procedures in patients with suspicion

of pulmonary hypertension – experiences of a tertiary center. *Postepy w Kardiologii Interwencyjnej*, 13(4):295–301, 2017.

[48] Bajc M., Neilly J. B., Miniati M., Schuemichen C., Meignan M., and Jonson B. EANM guidelines for ventilation/perfusion scintigraphy: Part 1. Pulmonary imaging with ventilation/perfusion single photon emission tomography. *European Journal of Nuclear Medicine and Molecular Imaging*, 36(8):1356–1370, 2009.

[49] Dolovich M. A. Influence of inspiratory flow rate, particle size, and airway caliber on aerosolized drug delivery to the lung. *Respiratory Care*, 45(6):597–608, 2000.

[50] Roach P. J., Bailey D. L., and Harris B. E. Enhancing Lung Scintigraphy With Single-Photon Emission Computed Tomography. *Seminars in Nuclear Medicine*, 38(6):441–449, 2008.

[51] Jögi J., Jonson B., Ekberg M., and Bajc M. Ventilation-perfusion SPECT with 99mTc-DTPA versus Technegas: a head-to-head study in obstructive and nonobstructive disease. *Journal of nuclear medicine : official publication, Society of Nuclear Medicine*, 51(5):735–741, 2010.

[52] Burch W. M., Sullivan P. J., and McLaren C. J. Technegas - a new ventilation agent for lung scanning. *Nuclear Medicine Communications*, 7(12):865–871, 1986.

[53] Oberdörster G. Pulmonary effects of inhaled ultrafine particles. *International Archives of Occupational and Environmental Health*, 74(1):1–8, 2000.

[54] Senden T. J., Moock K. H., Gerald J. F., Burch W. M., Browitt R. J., Ling C. D., and Heath G. A. The physical and chemical nature of technegas. *Journal of Nuclear Medicine*, 38(8):1327–1333, 1997.

[55] Lemb M., Oei T. H., Eifert H., and Günther B. Technegas: a study of particle structure, size and distribution. *European Journal of Nuclear Medicine*, 20(7):576–579, 1993.

[56] Peltier P., De Faucal P., Chetanneau A., and Chatal J. F. Comparison of technetium-99m aerosol and krypton-81m in ventilation studies for the diagnosis of pulmonary embolism. *Nuclear Medicine Communications*, 11(9):631–638, 1990.

[57] Bajc M., Schümichen C., Grüning T., Lindqvist A., Le Roux P. Y., Alatri A., Bauer R. W., Dilic M., Neilly B., Verberne H. J., Delgado Bolton R. C., and Jonson B. EANM guideline for ventilation/perfusion single-photon emission computed tomography (SPECT) for diagnosis of pulmonary embolism and beyond. *European Journal of Nuclear Medicine and Molecular Imaging*, 46(12):2429–2451, 2019.

[58] Taplin G. V., Johnson D. E., Dore E. K., and Kaplan H. S. Lung photoscans with macroaggregates of human serum radioalbumin: Experimental basis and initial clinical trials. *Health Physics*, 10(12):1219–1227, 1964.

[59] Heck L. L. and Duley J. W. Statistical considerations in lung imaging with 99Tc(m) albumin particles. *Radiology*, 113(3 I):675–679, 1974.

[60] Palmer J., Bitzén U., Jonson B., and Bajc M. Comprehensive ventilation/perfusion SPECT. *Journal of Nuclear Medicine*, 42(8):1288–1294, 2001.

[61] Jögi J., Palmer J., Jonson B., and Bajc M. Heart failure diagnostics based on ventilation/perfusion single photon emission computed tomography pattern and quantitative perfusion gradients. *Nuclear Medicine Communications*, 29(8):666–673, 2008.

[62] Schild H. H. *MRI made easy (...well almost)*. Schering, 1990.

[63] Schulz-Menger J., Bluemke D. A., Bremerich J., Flamm S. D., Fogel M. A., Friedrich M. G., Kim R. J., Von Knobelsdorff-Brenkenhoff F., Kramer C. M., Pennell D. J., Plein S., and Nagel E. Standardized image interpretation and post processing in cardiovascular magnetic resonance: Society for Cardiovascular Magnetic Resonance (SCMR) Board of Trustees Task Force on Standardized Post Processing. *Journal of Cardiovascular Magnetic Resonance*, 15(1):1–19, 2013.

[64] Nayler G. L., Firmin D. N., and Longmore D. B. Blood flow imaging by cine magnetic resonance. *Journal of Computer Assisted Tomography*, 10(5):715–722, 1986.

[65] Arheden H., Saeed M., Törnqvist E., Lund G., Wendland M. F., Higgins C. B., and Ståhlberg F. Accuracy of segmented MR velocity mapping to measure small vessel pulsatile flow in a phantom simulating cardiac motion. *Journal of Magnetic Resonance Imaging*, 13(5):722–728, 2001.

[66] Nayak K. S., Nielsen J. F., Bernstein M. A., Markl M., Gatehouse P. D., Botnar R. M., Saloner D., Lorenz C., Wen H., Hu B. S., Epstein F. H., Oshinski J. N., and Raman S. V. Cardiovascular magnetic resonance phase contrast imaging. *Journal of Cardiovascular Magnetic Resonance*, 17(1):1–26, 2015.

[67] Srichai M. B., Lim R. P., Wong S., and Lee V. S. Cardiovascular applications of phase-contrast MRI. *American Journal of Roentgenology*, 192(3):662–675, 2009.

[68] Borgquist R., Carlsson M., Markstad H., Werther-Evaldsson A., Ostenfeld E., Roijer A., and Bakos Z. Cardiac Resynchronization Therapy Guided by Echocardiography, MRI, and CT Imaging: A Randomized Controlled Study. *JACC: Clinical Electrophysiology*, 6(10):1300–1309, 2020.

[69] White J. A., Yee R., Yuan X., Krahn A., Skanes A., Parker M., Klein G., and Drangova M. Delayed Enhancement Magnetic Resonance Imaging Predicts Response to Cardiac Resynchronization Therapy in Patients With Intraventricular Dyssynchrony. *Journal of the American College of Cardiology*, 48(10):1953–1960, 2006.

[70] Alonso C., Leclercq C., Victor F., Mansour H., De Place C., Pavin D., Carré F., Mabo P., and Daubert J. C. Electrocardiographic predictive factors of long-term clinical improvement with multisite biventricular pacing in advanced heart failure. *American Journal of Cardiology*, 84(12):1417–1421, 1999.

[71] Molhoek S. G., Bax J. J., Boersma E., Van Erven L., Bootsma M., Steendijk P., Van Der Wall E. E., and Schalij M. J. QRS duration and shortening to predict clinical response to cardiac resynchronization therapy in patients with end-stage heart failure. *PACE - Pacing and Clinical Electrophysiology*, 27(3):308–313, 2004.

[72] Stellbrink C., Breithardt O. A., Franke A., Sack S., Bakker P., Auricchio A., Pochet T., Salo R., Kramer A., and Spinelli J. Impact of cardiac resynchronization therapy using hemodynamically optimized pacing on left ventricular remodeling in patients with congestive heart failure and ventricular conduction disturbances. *Journal of the American College of Cardiology*, 38(7):1957–1965, 2001.

[73] Rudski L. G., Lai W. W., Afilalo J., Hua L., Handschumacher M. D., Chandrasekaran K., Solomon S. D., Louie E. K., and Schiller N. B. Guidelines for the Echocardiographic Assessment of the Right Heart in Adults: A Report from the American Society of Echocardiography. Endorsed by the European Association of Echocardiography, a registered branch of the European Society of Cardiology, and. *Journal of the American Society of Echocardiography*, 23(7):685–713, 2010.

[74] Carlsson M., Heiberg E., Toger J., and Arheden H. Quantification of left and right ventricular kinetic energy using four-dimensional intracardiac magnetic resonance imaging flow measurements. *American Journal of Physiology - Heart and Circulatory Physiology*, 302(4):H893–900, 2012.

[75] Ugander M., Jense E., and Arheden H. Pulmonary intravascular blood volume changes through the cardiac cycle in healthy volunteers studied by cardiovascular magnetic resonance measurements of arterial and venous flow. *Journal of Cardiovascular Magnetic Resonance*, 11(1), 2009.

[76] Ugander M., Kanski M., Engblom H., Götberg M., Olivecrona G. K., Erlinge D., Heiberg E., and Arheden H. Pulmonary blood volume variation decreases after myocardial infarction in pigs: A quantitative and noninvasive MR imaging measure of heart failure. *Radiology*, 256(2):415–423, 2010.

[77] Kanski M., Arheden H., Wuttge D. M., Bozovic G., Hesselstrand R., and Ugander M. Pulmonary blood volume indexed to lung volume is reduced in newly diagnosed systemic sclerosis compared to normals - A prospective clinical cardiovascular magnetic resonance study addressing pulmonary vascular changes. *Journal of Cardiovascular Magnetic Resonance*, 15(86):1–8, 2013.

[78] Carlsson M., Ugander M., Mosén H., Buhre T., and Arheden H. Atrioventricular plane displacement is the major contributor to left ventricular pumping in healthy adults, athletes, and patients with dilated cardiomyopathy. *American Journal of Physiology - Heart and Circulatory Physiology*, 292(3):1452–9, 2007.

[79] Steding-Ehrenborg K., Carlsson M., Stephensen S., and Arheden H. Atrial aspiration from pulmonary and caval veins is caused by ventricular contraction and secures 70% of the total stroke volume independent of resting heart rate and heart size. *Clinical Physiology and Functional Imaging*, 33(3):233–240, 2013.

[80] Ostenfeld E., Stephensen S. S., Steding-Ehrenborg K., Heiberg E., Arheden H., Rådegran G., Holm J., and Carlsson M. Regional contribution to ventricular stroke volume is affected on the left side, but not on the right in patients with pulmonary hypertension. *International Journal of Cardiovascular Imaging*, 32(8):1243–1253, 2016.

[81] Heiberg E., Sjögren J., Ugander M., Carlsson M., Engblom H., and Arheden H. Design and validation of Segment - freely available software for cardiovascular image analysis. *BMC Medical Imaging*, 10(1):1–13, 2010.

[82] Guazzi M. Alveolar Gas Diffusion Abnormalities in Heart Failure. *Journal of Cardiac Failure*, 14(8):695–702, 2008.

[83] Friedman W. F. and Braunwald E. Alterations in regional pulmonary blood flow in mitral valve disease studied by radioisotope scanning. A simple nontraumatic technique for estimation of left atrial pressure. *Circulation*, 34(3):363–376, 1966.

[84] West J. B., Dollery C. T., and Heard B. E. Increased Vascular Resistance in the Lower Zone of the Lung Caused By Perivascular Œdema. *The Lancet*, 284(7352):181–183, 1964.

[85] Jögi J., Ekberg M., Jonson B., Bozovic G., and Bajc M. Ventilation/perfusion SPECT in chronic obstructive pulmonary disease: An evaluation by reference to symptoms, spirometric lung function and emphysema, as assessed with HRCT. *European Journal of Nuclear Medicine and Molecular Imaging*, 38(7):1344–1352, 2011.

[86] Mohsenifar Z., Amin D. K., and Shah P. K. Regional distribution of lung perfusion and ventilation in patients with chronic congestive heart failure and its relationship to cardiopulmonary hemodynamics. *American Heart Journal*, 117(4):887–891, 1989.

[87] Pistolesi M., Miniati M., Bonsignore M., Andreotti F., Ricco G. D., Marini C., Rindi M., Biagini A., Milne E. N., and Giuntini C. Factors affecting regional pulmonary blood flow in chronic ischemic heart disease. *Journal of Thoracic Imaging*, 3(3):65–72, 1988.

[88] Gilday D. L. and James A. E. Lung scan patterns in pulmonary embolism versus those in congestive heart failure and emphysema. *The American journal of roentgenology, radium therapy, and nuclear medicine*, 115(4):739–750, 1972.

[89] Andersen A. and Andersen M. J. Elevated left atrial pressure in heart failure: should you relieve the pressure? *Trends in Cardiovascular Medicine*, 20(Epub ahead of print): 30131–6, 2020.

[90] Vitorelli A., Ferro Lazzi M., Penco M., Ciciarello F., Fedele F., and Dagianti A. PVF velocity pattern in patients with heart failure: Transesophageal echocardiographic assessment. *Cardiology (Switzerland)*, 88(6):585–594, 1997.

[91] Smiseth O. A., Thompson C. R., Lohavanichbutr K., Ling H., Abel J. G., Miyagishima R. T., Lichtenstein S. V., and Bowering J. The pulmonary venous systolic flow pulse - Its origin and relationship to left atrial pressure. *Journal of the American College of Cardiology*, 34(3):802–809, 1999.

[92] Karatzas N. B. and Lee G. J. Propagation of blood flow pulse in the normal human pulmonary arterial system. Analysis of the pulsatile capillary flow. *Circulation research*, 25(1):11–21, 1969.

Printed by Media-Tryck, Lund 2021 NORDIC SWAN ECOLABEL 3041 0903

About the author

Mariam Al-Mashat is born on April 6th, 1990. She was raised together with her two younger brothers in a very caring and loving family. She graduated from Malmö University, Sweden in 2011 as a Biomedical laboratory scientist with a specialization in Clinical physiology (Technologist). Two years after, Mariam graduated from Örebro University, Sweden with a master's degree in Medicine. Mariam started to work at the department of Clinical Physiology and Nuclear Medicine at Skåne University Hospital in Lund Sweden in 2011 and became a member of the research group, Lund Cardiac MR group, in 2012. In this group, Mariam's journey towards accomplishing her dream of obtaining a PhD degree started.

"Spring's breaths" Artist: Mona Taqi

Photographer: Sarah Khafagi

LUND UNIVERSITY

FACULTY OF MEDICINE

Department of Clinical Physiology

Lund University, Faculty of Medicine
Doctoral Dissertation Series 2021:01
ISBN 978-91-8021-007-2
ISSN 1652-8220